Johannes Kepler University Linz

University of South Bohemia in České Budějovice

^{13}C Magnetic Resonance Spectroscopy Measurements of Glutaminase Activity Using Hyperpolarized ^{13}C-Labeled Glutamine

Master Thesis

to obtain an academic degree

Master of Science (MSc)

in master studium program

Joint Master Programme Biological Chemistry

AUTHOR:

Bc. Eugen Kubala, BSc

SUPERVISORS:

Univ.-Prof. Dr. Norbert Müller

Dr. Marion I. Menzel

Linz, May 2013

ANNOTATION

Nuclear magnetic polarization decays fast in the liquid state during the transfer of glutamine in Earth's magnetic field as observed by substantial T_1 shortening due to scalar coupling relaxation (type II) of ^{13}C coupled to fast-relaxing quadrupolar ^{14}N in the glutamineâs amide group. Hyperpolarization can be retained by using either a ^{15}N-labeled amide or by applying a strong magnetic field during sample transfer.

ABSTRACT

Detection of abnormal metabolic fluxes or unusual accumulation of metabolites could be used to monitor the predisposition to cancer in humans. Imaging can not only support an initial diagnosis, but also monitor progress in terms of staging, restaging, treatment response, and identification of recurrence, both at the primary tumor and at distant metastatic sites. Due to change in tumor metabolism elevated glutamine cellular uptake and its metabolism may act a marker of tumor growth and cell proliferation. Metabolic magnetic resonance imaging with hyperpolarized ^{13}C-labelled substances (^{13}CMMR) allows non–invasive investigation of *in vivo* metabolism. Using ^{13}CMMR, metabolism of ^{13}C-glutamine can be tracked *in vivo* in real time and the glutamine accumulation can localize the tumor. While working on [5-^{13}C]glutamine hyperpolarization, fast liquid-state polarization decay during the transfer through Earth's low magnetic field to the MRI scanner was observed. This behavior could be hypothetically explained by substantial T_1 shortening due to a relaxation through scalar coupling relaxation (type II) of ^{13}C coupled to fast-relaxing quadrupolar ^{14}N in the glutamine's amide group. This contribution is only effective in Earth's low magnetic fields ($> 800~\mu$T) and prevents the use of molecules bearing the ^{13}C-^{14}N-amide group as hyperpolarized MRS/MRI probes. The experimental results show that high hyperpolarization levels can be retained using either a ^{15}N-labeled amide or by applying a strong magnetic field during transfer of the sample from the polarizer to the MRI scanner.

PUBLICATIONS

Some ideas and figures have appeared previously in the following publication:

E. Chiavazza, E. Kubala, C.V. Gringeri, S. Düwel, M. Durst, R.F. Schulte, M.I. Menzel. (2013) **Earth's magnetic field enabled scalar coupling relaxation of ^{13}C nuclei bound to fast-relaxing quadrupolar ^{14}N in amide groups**, *Journal of Magnetic Resonance*, Vol. 227, pp. 35-38, ISSN 1090-7807, 10.1016/j.jmr.2012.11.016.

"But I don't want to go among mad people," Alice remarked.
"Oh, you can't help that," said the Cat:
"we're all mad here. I'm mad. You're mad."
"How do you know I'm mad?" said Alice.
"You must be," said the Cat, "or you wouldn't have come here."

— Lewis Carroll [1]

ACKNOWLEDGMENTS

Thank You.

CONTENTS

LIST OF FIGURES

LIST OF TABLES

ACRONYMS

ACL   ATP citrate lyase

ALT   Alanine aminotransferase

AST   Aspartate aminotransferase

ATP   Adenosine triphosphate

α-KG   α-ketoglutarate

BNMRZ   Bavarian NMR Center

cDNA   Complementary DNA

CI   Confidence intervals

Co   Cobalt

CO$_2$ Carbon dioxide

Cu   Copper

DMSO   Dimethyl sulfoxide

DNA   Deoxyribonucleic acid

DNP   Dynamic nuclear polarization

D$_2$O   Heavy water (deuterium oxide)

EDTA   Ethylenediaminetetraacetic acid

EPR   Electron paramagnetic resonance

Fe   Iron

FH   Fumarase

FID   Free induction decay

GAD   Glutamate decarboxylase

Gd   Gadolinium

GdDOTA   Gadolinium-tetraazacyclododecanetetraacetic acid

GEGR   GE Global Research

GLDH   Glutamate dehydrogenase

Gln   Glutamine

GLS   Glutaminase

Glu   Glutamic acid

HCC   Hepatocellular carcinoma

HCl   Hydrochloric acid

HF   Hydrofluoric acid

HIF   Hypoxia-inducible factor

HNO_3 Nitric acid

HR-ICP-MS High Resolution Inductively Coupled Plasma Mass Spectrometry

H_2O Water

H_3O^+ Hydronium

IDH   Isocitrate dehydrogenase

K_2CO_3 Potassium carbonate

LDH   Lactate dehydrogenase

lHe   Liquid Helium

lN$_2$ Liquid Nitrogen

MMR   Metabolic magnetic resonance

Mn   Manganese

Mo   Molybdenum

MR   Magnetic resonance

MRI   Magnetic resonance imaging

mRNA   Messenger RNA

MRS   Magnetic resonance spectroscopy

NaOH   Sodium hydroxide

NH_3 Ammonia

Ni   Nickel

NMR   Nuclear magnetic resonance

OH^- Hydroxyl

OX063 methyl-tris[8-carboxy-2,2,6,6-tetrakis[(2-hydroxyethyl]benzo[1,2-d:4,5-d']bis[1,3]dithiol-4-yl

PCA   2-pyrrolidone-5-carboxylicacid

PDH   Pyruvate dehydrogenase

pGlu   Pyroglutamic acid

PHIP   Parahydrogen-induced polarization

pK_a Acid dissociation constant

PTFE   Polytetrafluoroethylene

PTMs   Posttranslational modifications

RF   Radio-frequency

RNA   Ribonucleic acid

SDH   Succinate dehydrogenase

TCA   Tricarboxylic acid

TEMPO (2,2,6,6-tetramethylpiperidin-1-yl)oxidanyl

Ti   Titanium

TPN   Total parenteral nutrition

TRIS   Tris(hydroxymethyl)aminomethane

TUM   Technical University Munich

T_1 Longitudinal relaxation time

$T_2{}^*$ Decay constant of the FID instrumentally dependant

VHL   Von Hippel–Lindau tumor suppressor

VTI   Variable temperature insert

Zn   Zinc

Part I

INTRODUCTION

I started where the last man left off.

— Thomas A. Edison

GLUTAMINE

This year it has been exactly 130 years since the amino acid glutamine (Gln, Q) has been first described. It was isolated from the beetroots by E. Schulze and E. Bosshard in 1883 [2]. Since then it was found that glutamine is the most abundant naturally occurring amino acid in the human plasma with concentration of $600 - 800$ μmol/L, and that it exhibits extremely rapid cellular turnover rates [3, 4].

Although in most biochemistry textbooks glutamine is nowadays still classified as non–essential due to the fact that it can be synthetized by almost any mammalian tissue, it appears essential for the viability and growth of cells maintained in tissue cultures [5]. Glutamine plays an important role as a substrate for several metabolic pathways such as renal ammonia production [6], hepatic gluconeogenesis [7], and modulation of muscle protein turnover [8]. It also serves as a metabolic fuel for enterocytes [9, 10], metabolic precursor in nucleotide, glucose, and amino sugar biosynthesis, and it is important for glutathione homeostasis and protein synthesis [11]. Moreover, the growth of proliferating cells such as fibroblasts, lymphocytes and enterocytes relies heavily on glutamine as an oxidative energy source. The nitrogen-rich character and unique metabolism of this amino acid allows it to serve as the major interorgan ammonia shuttle. Glutamine also supports tissue homeostasis by participation in intercellular substrate cycles in the brain and liver. It also plays an important role in fetal-placental nutrient exchange [12], and helps to maintain the integrity of the gut mucosa in postoperative patients [13, 14].
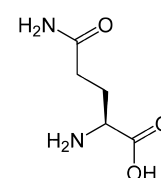
L-*glutamine*

1.1 GLUTAMINE INSTABILITY AND DEGRADATION

Even though glutamine does not show any rapid conversion to other compounds in solid state at room temperature [15], it is relatively unstable in solutions and very likely releases ammonia during its degradation. By contrast, the similar amino acid glutamate (Glu) seems to be quite stable under the same conditions (Fig. 1). This suggests that the ammonia released from glutamine is mainly due to the deamidation of the side-chain amide group [16]. Glutamine very likely undergo hydrolysis to glutamic acid (Glu) and ammonia due to the pH of the environment [17], while at higher temperature, the amino-group of glutamine is labile and yields to conversion to pyroglutamic acid (pGlu) also known as 2-pyrrolidone-5-carboxylicacid (PCA) or 5-oxopyrrolidine-2-carboxylic acid [18].
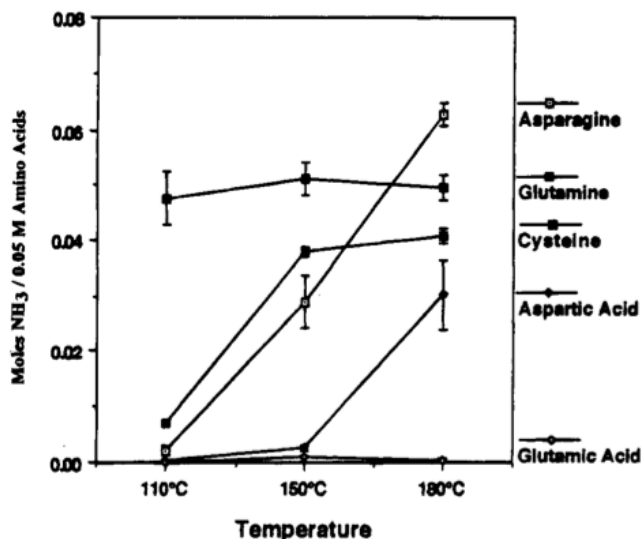
Figure 1: Molar yield of ammonia generation at three different temperatures. Amino acids (0.05M) were reacted at 110, 150, and 180°C for 2 hours at pH 8 [16].

1.1.1 *Degradation due to the pH environment*

The pH of the solution plays an important role in the stability of glutamine. Glutamine degrades very rapidly when the pH of the solution is below 1.5 and above 12.5. It undergoes hydrolysis into glutamic acid and ammonia [15]. Glutamic acid is particularly stable in very acidic or very alkaline conditions, and therefore it cannot be converted into pyroglutamic acid under such conditions [15, 19]. The rate of the degradation decreases with the pH approaching neutral conditions.
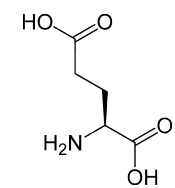
There are several mechanisms that drive the degradation of glutamine into glutamic acid or pyroglutamic acid (Fig. 2.1). In acidic conditions the degradation is rapid and the rate decreases with an increase in pH. This indicates that the cationic glutamine species undergoes specific hydrogen-ion catalysis (Fig. 2.1$_d$) and water hydrolysis (Fig. 2.1$_b$). The degradation of glutamine neutral species is mainly due to the hydrolysis by water molecules (Fig. 2.1$_a$). In the alkaline conditions, the rate indicates a specific hydroxide-ion catalysis (Fig. 2.1$_e$) and water hydrolysis (Fig. 2.1$_c$) of the glutamine anionic species [20].

1.1.2 *Degradation due to the temperature conditions*

If the solution is heated, glutamine tends to undergo a reaction into pyroglutamic acid and ammonia. This conversion has been well documented by Foreman et al. already in 1914, and later by Mahdi et al. (1961), and Clydesane et al. (1972) [21, 22, 23]. Arii et al. (1999) confirmed theirs observation, when they described a close agreement between the loss of the glutamine and the appearance of pyroglutamic acid under all pH conditions (pH = 1.93, 6.41 and 11.01) at 70°C [20].

L-*glutamic acid*
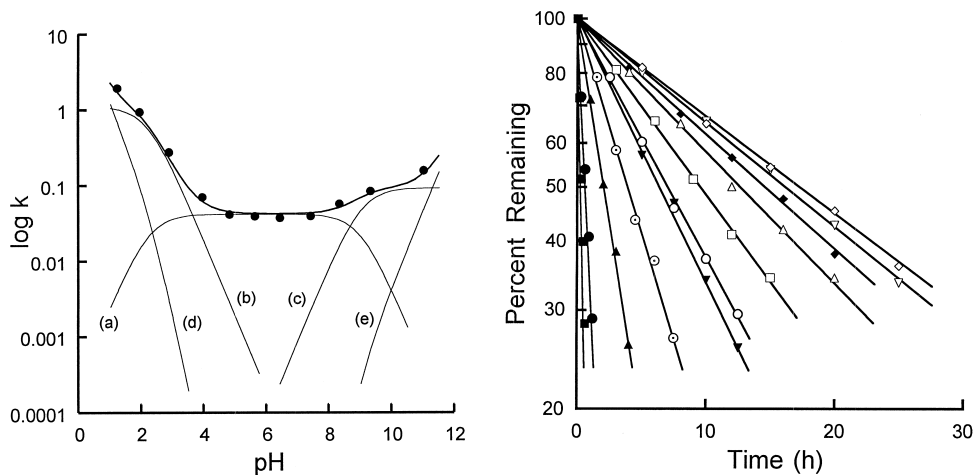
2.1: pH-rate profile for the degradation of L-glutamine in aqueous solution at 70°C.

2.2: Apparent first-order plot of the degradation of glutamine at 70°C in buffer solution.

Figure 2: Influence of the pH profile on the degradation of L-glutamine in aqueous solution at 70°C. Notation for Fig. 2.1: (a) water-catalyzed degradation of neutral species, (b) water-catalyzed degradation of cationic species, (c) water-catalyzed degradation of anionic species, (d) hydrogen-ion-catalyzed degradation of cationic species, and (e) hydroxide-ion-catalyzed degradation of anionic species. Notation for the pH values of the solution in for Fig. 2.2: (■) 1.21, (●) 1.93, (▲) 2.87, (▼) 3.93, (◆) 4.80, (▽) 5.61, (◇) 6.41, (△) 7.39, (□) 8.31, (○) 9.31, (⊙) 11.01 [20].

Glutamine's maximum stability was observed in media with neutral pH conditions, however, under highly acidic or highly alkaline conditions the conversion to Glu or pGlu was almost complete. The amount of glutamine residue after 60 minutes boiling was never greater than 35%. At 100°C glutamine was converted into pyroglutamic or glutamic acids depending upon the pH value [15].

At extreme conditions (pH 0 and pH 14) glutamine degraded completely into glutamic acid, which appeared almost exclusively. When pH values ranged from 0 to 3 on one hand and from 10 to 14 on the other hand, equilibrium was noticed between resulting glutamic acid and pyroglutamic acid. This resulting phenomenon was described by Airaudo et al. in 1987. They described that under non–extreme pH (pH 3 – 10; 100°C) glutamine showed a more complex behaviour resulting in the appearance of glutamine, glutamic acid and pyroglutamic acid mixtures when the pH value was favourable. They interpreted these results in two possible explanations. Either glutamine was transformed into the mixture of Glu and pGlu depending upon the pH, or the glutamine underwent a two–step conversion. First the glutamine hydrolyzed into glutamic acid, whatever the pH value was, and then glutamic acid underwent reaction into pyroglutamic acid if the acidity or alkalinity of the medium was not extreme. The fact that after boiling no glutamic acid was found in pH region 3 – 10, whereas in the first study this nutrient was stable between pH 5 and pH 8, seems to favour the first interpretation. When heated to 135°C the results
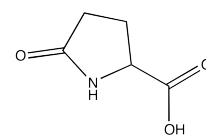
Pyroglutamic acid

observed were very similar to ones at 100°C, but they were more marked because the experimental conditions were more severe. However, glutamic acid and pyroglutamic acid never underwent a reverse reaction into glutamine, but were reversibly converted into one another [15].

The activation energy for degradation of glutamine was determined to be 9.87×10^4 J mol^{-1} and the frequency factor (*log A*) was determined to be 31.5 h^{-1} [20].

1.1.3   *Degradation of glutamine in peptides*

Non–enzymatic deamidation of glutamine's side-chain amide group in peptides has been observed by several studies [25, 26, 27, 28]. It belongs to one of the most important protein posttranslational modifications (PTMs), which contributes to ageing and diseases such as celiac disease, urinary tract infection, cataract formation, cancer, and neurodegenerative diseases (e.g. Alzheimer's, Huntington's, and Parkinson's diseases). In every day life this reaction also affects the purity and the "shelf life" of pharmaceutical products [29]. However, several studies have shown that glutamine stability can be increased if the correct pharmaceutical techniques are followed. At a pH just below neutrality, the concentration of glutamine in total parenteral nutrition (TPN) solution decreased by 5% per day at 37°C [30]. At room temperature, glutamine degradation was $0.7 - 0.9\%$ per day in different parenteral solutions [31].

Figure 3: First-order kinetic plot of degradation of glutamine into PCA in sodium acetate buffer solutions with an acetate ion concentration of 0.073 mol L^{-1} and pH 3, 4, 5, and 6 [24].

1.2   GLUTAMINE UPTAKE INTO THE CELL

Today it is widely accepted that the transport of glutamine across the plasma and mitochondrial membrane plays a crucial role in the control of its metabolism [32]. Glutamine, as all other amino acids, is transported into the mammalian cells by a group of transporters, which can be divided into two categories: Na$^+$-dependent and Na$^+$-independent. Na$^+$-dependent glutamine transporters include: Systems ASC (or B^o), B$^{o,+}$, y$^+$L, A and N. On the other hand Na$^+$-independent transporters include: Systems L, b$^{o,+}$ and n [12]. There is no transporter that is absolutely specific for glutamine only. In each case glutamine is just one of the amino acids recognized and transported by a particular transporter [33].

For our purposes we will focus only on transporters belonging into Na$^+$-dependent group: system N (SNAT3, SNAT5) and system A (SNAT2), because these are the transporters responsible for the transport of the glutamine in the healthy hepatocytes

[32]. However, we will also describe the system ASC (ASCT2) because it is mainly responsible for glutamine transport in hepatocellular carcinoma [34, 35].

1.2.1   *System N*

System N plays a major role in hepatic glutamine transport. It includes two subtypes SNAT3 and SNAT5, formally referred as SN1 and SN2. Both subtypes have very narrow substrate specificity of glutamine, alanine, asparagine, and histidine, with high affinity for glutamine and histidine [12, 36, 37, 38]. Human SNAT3 protein is 90% identical to rat SNAT3, and 89% identical to mouse SNAT3 [12].

In rodents, SNAT3 is mainly expressed in hepatocytes [36], the pericentral region of liver [37], but also in skeletal muscle [39], tubules in the medulla of kidney [37], heart, basolateral and brush border membrane vesicles [40], basolateral membranes of cortical tubule cells [41], neurones (N^n) [42], and brain glial cells [43].

The mechanism of the SNAT3 strongly depends on Na^+/H^+ counter-transport mechanism [38, 43], which makes it pH sensitive in physiologic range, with reduced activity at acidic pH [36, 44, 45]. Fei et al. described that SNAT3 is electrogenic and with two Na^+ molecules transported with glutamine inward coupled to H^+ efflux outwards the cell [38]. Other studies proposed electroneutral transport with one Na^+ being transported with one glutamine molecule inwards and one H^+ ion moving in the opposite direction [46, 47]. SNAT3 is able to mediate both glutamine uptake and release. The direction of the transport depends on membrane electrical potential, Na^+ and pH gradient, and transmembrane glutamine concentration gradient [38, 43].

SNAT5 (SN2), like SNAT3, catalyzes uptake of glutamine with Na^+ in exchange for H^+, however, its physiological function is not yet clear [33]. It has slightly different substrate specificity than SNAT3. It transports glutamine, alanine, asparagine, glycine, and serine [48] and is expressed more in the periportal hepatocytes in rat liver, while SNAT3 was preferentially expressed in the pericentral region [49].

1.2.2   *System A*

The system A includes two subtypes SNAT1 (ATA1) and SNAT2 (ATA2), however only SNAT2 is incorporated in the glutamine transport in liver. Its cDNA was isolated in rat neurons [50], skeletal muscle [51], and glutamatergic neurons [52]. The SNAT2 mRNA was expressed in all tissues examined, including brain, liver, heart, kidney, colon, small intestine, lung, muscle, spleen, stomach, testis and placenta [53]. In rat brain, both SNAT1 and SNAT2 are restricted to neurones and are absent in astrocytes [52, 54]. The human SNAT2 is 88% identical to rat homologue [53]. Similar to SNAT3 and ASCT2, transport mediated by rat SNAT2 (specifically Na^+ binding) is sensitive to the membrane potential [52], but it is unclear whether the same is true for SNAT1.

1.2.3 *System ASC (B⁰)*

Even though ASCT2 (in human also referred as ATB⁰) is not incorporated in glutamine transport in healthy hepatocytes, it is a very important part of the glutamine metabolism in hepatocellular carcinoma (HCC). Glutamine uptake by hepatoma cells exceeds rates observed in normal hepatocytes more than 30-fold. This is possible due to the expression of high affinity glutamine transporters of the ASCT2 family [34, 35].

ASCT2 is normally undetectable in the healthy hepatocytes [55], however, it is normally expressed in placenta, lung, kidney, pancreas, skeletal muscle, kidney proximal tubule, and intestinal epithelia [56, 57, 58]. ASCT2 expression was also found in glia, but interestingly not in neurons [59].

ASCT2 takes up glutamine with high affinity, however, it transports also a wide range of other zwitterionic amino acids such as alanine, asparagine, cysteine, serine, threonine as well as bulky/branch-chained amino acids such as leucine, valine, and methionine to a lesser degree [57, 60].

At the amino acid level, rat ASCT2 is 83% identical to mouse ASCT2 and 76% identical to human ATB⁰ [59]; mouse ASCT2 shares 79% identity with human ATB⁰, whereas rabbit and human ATB⁰ are 85% identical [56]. Although they are minor differences between clones from various species in amino acid transport specificity, the originally held view that ATB⁰ and ASCT2 clones represented different transporters is no longer valid [33]. These broad-specificity transporters are now all commonly referred to as ASCT2.

The ASCT2 transport mechanism of action is not yet clear. First observation of ASCT2 in rabbit intestine proposed a mechanism of electrogenic Na^+-substrate uptake [56], however, one year later Torrents et al. proofed that the mechanism involves a Na^+-dependent exchange of intracellular for extracellular amino acids, effectively serving to equilibrate cytoplasmic amino acid pools [61]. A study using mouse brain ASCT2 concluded that the amino acid exchange was obligatory and that exchange of Na^+ ions also occurred [62]. This transporter can therefore mediate either glutamine uptake or release [33, 59].

On the other hand studies on human ASCT2 showed that glutamine uptake is electroneutral, with one amino acid and one Na^+ ion transported inwardly and with no evidence for the opposite movement of either K^+ or H^+ [63]. In a later paper, using the ASCT2 from human small intestine it was proposed that ASCT2 catalyzed an exchange of external for internal amino acids that was completely dependent on Na^+ ions [58]. Since all these studies were performed using clones of different origins it is not impossible that relatively small differences in amino acid sequence in these clones can produce different behaviour when expressed in oocytes. However, whatever the situation in oocyte expression experiments was, glutamine uptake catalyzed by ASCT2 in hepatoma cells is highly concentrative and very largely Na^+-dependent [64].

1.3   GLUTAMINE METABOLISM

After uptake across the plasma membrane glutamine is hydrolyzed to glutamate and ammonium ions by enzyme glutaminase (GLS; EC 3.5.1.2). The hydrolysis of glutamine in mammalian tissues was first described by Krebs in 1935. In his article he proposed an hypotheses: *"There are at least two glutaminases distinguishable by their pH optima and their inhibitions by glutamic acid ("brain-type" and "liver-type")."* [65]. Nowadays we know that his hypotheses was correct. Two types of phosphate-dependent glutaminases are expressed in mammalian tissues: the "kidney-type" (referred by Krebs as a "brain-type") is found in most mammalian tissues, and the "liver-type", which is liver-specific and is linked functionally to the urea cycle [66]. Despite their differences both types catalyse the following reaction:
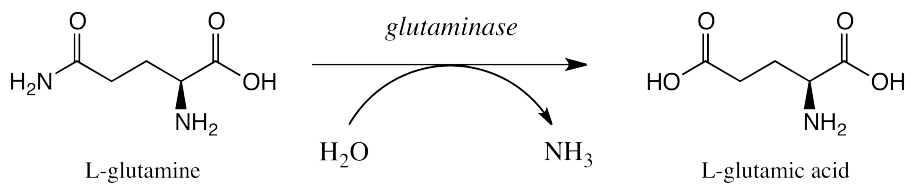
Figure 4: Simplified reaction of glutamine to glutamic acid catalyzed by glutaminase

1.3.1   *"Liver-type" glutaminase*

"Liver-type" glutaminase is encoded by the nuclear gene termed GLS2 and it is specifically expressed only in the liver tissue. It composes of four subunits each of 58 kDa. Interestingly it is activated by its end product ammonia [67, 68], with NH_3 being the activating species [69]. Ammonia formed by the glutaminase-catalyzed reaction again stimulates glutaminase activity, leading to an autoamplification of mitochondrial ammonia production. Most importantly, already physiological ammonia concentration (0.2 – 0.3 mM) stimulates glutaminase activity [70]. Mitochondrial swelling activates glutaminase as does an increase in pH [71, 72]. The formed ammonia from the amide group of glutamine is not released from the cell, but instead is fixed in urea [32].

1.3.2   *"Kidney-type" glutaminase*

"Kidney-type" glutaminase is encoded by the nuclear gene termed GLS1 and it is expressed in all mammalian tissues except liver. It composes of four subunits of 65 and 68 kDa. Differently from the "liver-type", the "kidney-type" glutaminase is not activated but <u>inhibited</u> by its end product glutamate and underlies regulation at the transcriptional level [32]. Most of the amide ammonia does not undergo further metabolism and is released from the cells as free ammonia. The end product glutamate (Glu) can be transaminated by aspartate and alanine aminotransferases (AST, ALT), oxidatively deaminated by glutamate dehydrogenase (GLDH), or decar-

boxylated by glutamate decarboxylase (GAD). The exact product is tissue specific [73].

1.4   THE ROLE OF GLUTAMINE IN CANCER

Unicellular organisms, such as microbes, are evolutionary under pressure to reproduce as quickly as possible when nutrients are available. Therefore their metabolic systems have evolved to supply nutrients including carbon, nitrogen, and free energy into generating the building blocks needed to produce a new cell.

By contrast, cells in multicellular organisms do not need to deal with lack of nutrients, since most are exposed to a constant supply of nutrients. Multicellular organisms require control systems that prevent aberrant individual cell proliferation. Uncontrolled proliferation is prevented by the mechanism of growth factors, which need to stimulate the cell for normal nutrients uptake. Cancer cells overcome this mechanism by acquiring genetic mutations that functionally alter receptor-initiated signaling pathways [75].

As a consequence of rapid proliferation cancer cells require a constant supply of building blocks to generate daughter cells. Most oncogenic pathways lead to changes in the cancer gene expression that facilitate nutrient uptake and reprogram metabolic
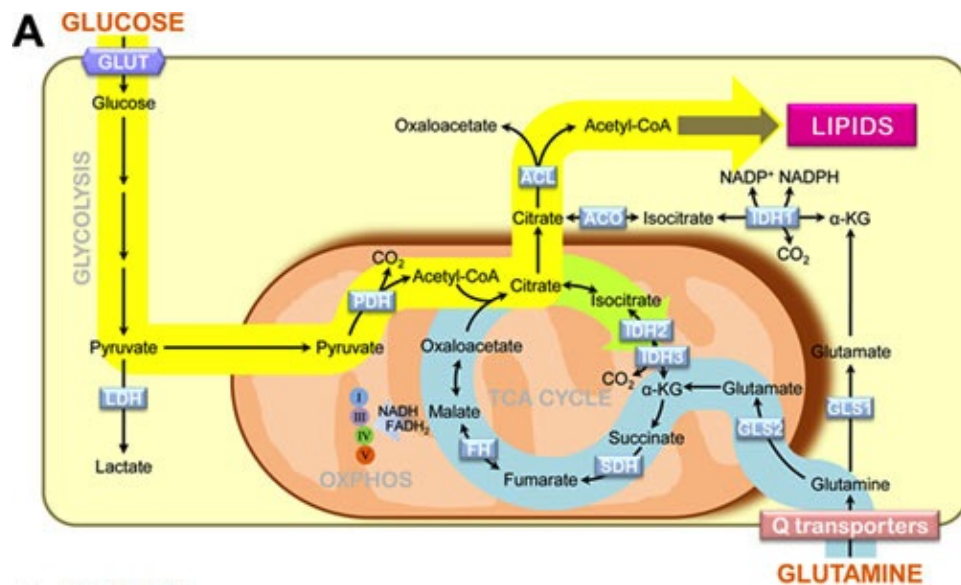
Figure 5: A lipid synthesis metabolism of healthy hepatocyte. When mitochondrial respiration is fully functional, glucose serves as a major carbon source for synthesis of acetyl-CoA – metabolic lipid precursor (indicated by the yellow path). The blue path indicates the oxidative glutamine metabolism (anaplerosis). The green path shows the metabolic pathway of citrate generated from glucose-derived acetyl-CoA and glutamine-derived oxaloacetate. Notation: LDH: Lactate dehydrogenase, PDH: Pyruvate dehydrogenase, ACL: ATP citrate lyase, SDH: Succinate dehydrogenase, FH: Fumarase, IDH: Isocitrate dehydrogenase, GLS: Glutaminase, α-KG: α-ketoglutarate, CO_2: Carbon dioxide [74].

processes to promote the utilization of nutrients for anabolism [75]. Actually most of the metabolites taken up by proliferating cells are not catabolized, but instead are used as building blocks during anabolic macromolecular synthesis. The catabolic reactions that fuel the growth and proliferation of the cells require two main substrates: glucose and glutamine [76, 77, 78, 79]. The mechanisms by which glutamine supports the cancer metabolism are not fully understood [74].

For rapid proliferation cancer cells require an increase of the glutamine uptake into the cell. Enhanced activity of the oncogenic transcription factor c-Myc increases the expression of the surface transporters ASCT2 and SNAT5 [80]. The ASCT2 transporter mediates the majority of glutamine uptake in human hepatoma [44, 81, 82], breast carcinoma [76] and colon carcinoma [56, 57, 82, 83]. For instance in hepatocellular carcinoma (HCC) glutamine uptake is up to 30-fold higher than in normal healthy hepatocytes [12, 73, 84].

The activity of the oncogenic transcription factor c-Myc also increases the glutamine metabolism. The c-Myc enhances the expression of the "kidney-type" glutaminase encoded by the GLS1 gene [80, 85]. Studies with rat hepatoma cells showed that, on cellular transformation, the "liver-type" isozyme is lost and is re-placed by the "kidney-type". Thanks to the alternation in uptake and expression of "kidney-type" isozyme of glutaminase hepatoma cells possess 6-fold higher glutaminase activity than healthy human liver cells [73].
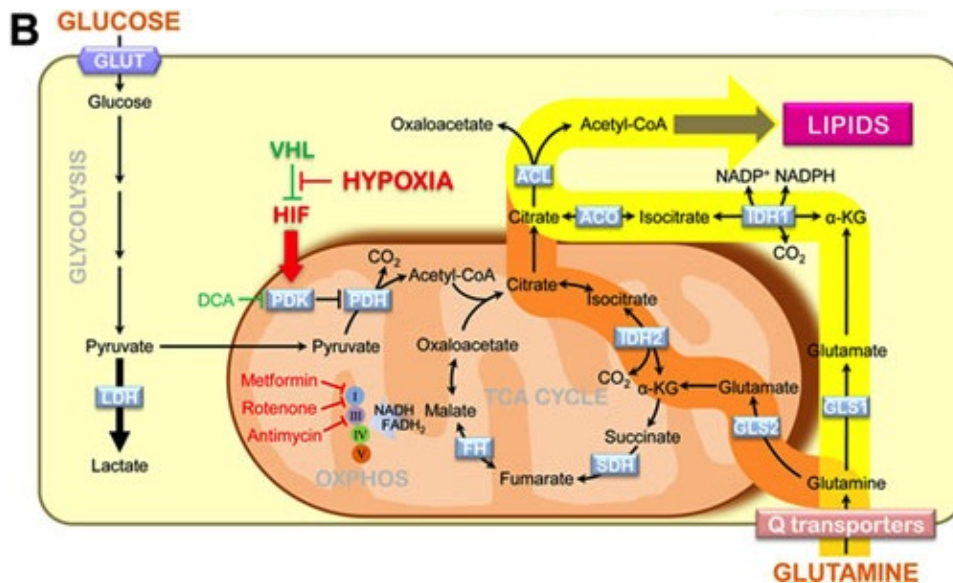
Figure 6: A lipid synthesis metabolism in hepatocellular carcinoma. Under conditions when mitochondrial respiration is limited for instance due to the stabilized Hypoxia–inducible factor (HIF) upon hypoxia, or Von Hippel–Lindau tumor suppressor (VHL) deletion, glutamine overtakes the role of the major carbon source for lipogenic acetyl-CoA either via cytoplasmic IDH1 (yellow path) or mitochondrial IDH2 (orange path). Notation: LDH: Lactate dehydrogenase, PDH: Pyruvate dehydrogenase, ACL: ATP citrate lyase, SDH: Succinate dehydrogenase, FH: Fumarase, IDH: Isocitrate dehydrogenase, GLS: Glutaminase, α-KG: α-ketoglutarate, CO_2: Carbon dioxide [74].

Since glutamine is a great source of nitrogen and carbon, this feature makes it a crucial nutrient during the cell proliferation. One route of glutamine catabolism involves its conversion to glutamate by glutaminase (GLS) in mitochondria. Glutamate is, in turn, deaminated to generate α-ketoglutarate. The remaining nitrogens from the glutamine's amino and amido group are either transferred to metabolic intermediates in the synthesis of nucleic acids, proteins, and hexosamines or released as ammonia. The α-ketoglutarate can enter the TCA cycle and keeps it turning when glucose-derived citrate is re-routed to the cytoplasm for the lipogenesis (Figure 5 – yellow path). This function of glutamine is referred as "anaplerosis", a process of restoring the cellular metabolic intermediate pools [74, 86]. Some cancer cells produce more than 50% of their adenosine triphosphate (ATP) by this metabolic pathway [78].

Even though glutamine is a great source for producing ATP, a boost in lipid synthesis is more critical for supporting the proliferation. During the rapid proliferation a hypoxia is a very common feature of cancer tissue. Under hypoxic conditions pyruvate entry into mitochondria is limited [87], therefore glutamine takes over the role of the major carbon source for lipogenesis via the reductive carboxylation route (Fig. 6 – yellow path). Since cancer cells prefer to generate lipids *de novo* rather than use them directly from their environment, this is the only possible metabolic pathway how to retain the same proliferation rate under hypoxia [74, 87].

Detection of abnormal metabolic fluxes or the accumulation of unusual metabolites could be used to monitor the predisposition to cancer in humans [88, 89]. Imaging can not only support an initial diagnosis but also monitor progress in terms of staging, restaging, treatment response, and identification of recurrence, both at the primary tumor and at distant metastatic sites [88].

MAGNETIC RESONANCE SPECTROSCOPY (MRS)

The basic principle of magnetic resonance imaging (MRI) is based on the behaviour of atomic nuclei in an external magnetic field. One of the fundamental physical properties of the atomic nucleus is the nuclear spin, which is described by the quantum number I. To be visible using the nuclear magnetic resonance (NMR) atomic nucleus must have a non-zero spin quantum number. This requirement fulfill for instance the isotopes such as ^{1}H, ^{3}He, ^{13}C, ^{14}N, ^{15}N, ^{31}P and ^{129}Xe.

Until recent time MRI has been restricted to ^{1}H. Not only that ^{1}H has higher sensitivity than any other nucleus in endogenous substances, it is also highly abundant in a very high concentration (about 80 M) in biological tissues.

Nuclei with spin quantum number $I = \frac{1}{2}$ (e. g. ^{1}H, ^{3}He, or ^{13}C) can orient themselves in two possible directions related to the external magnetic field: parallel ("spin up") or anti-parallel ("spin down"). The measurable final NMR signal is proportional to the population difference between the two possible orientation directions. Denoting the number of spins in the parallel and anti-parallel directions to the high magnetic field $N_{+\frac{1}{2}}$ and $N_{-\frac{1}{2}}$, respectively, the polarization P is by definition given as:

$$P = \frac{N_{+\frac{1}{2}} - N_{-\frac{1}{2}}}{N_{+\frac{1}{2}} + N_{-\frac{1}{2}}} \tag{1}$$

If the amount of nuclei with opposite direction is equal, the magnetic moments cancel, and result in zero macroscopic magnetization, and thus no NMR signal. However, under thermal equilibrium conditions, slightly higher energy is associated with the anti-parallel ($N_{-\frac{1}{2}}$) direction, and therefore it will be slightly smaller than $N_{+\frac{1}{2}}$ (see Figure 8: Thermal equilibrium). For a nucleus with spin quantum number $I = \frac{1}{2}$, the thermal equilibrium polarization P is given by:

$$P = \tanh\left(\frac{\gamma \hbar B_0}{2 k_B T}\right) \tag{2}$$

where *tanh* refers to the hyperbolic tangent, B_0 is the magnetic field strength, γ the gyromagnetic ratio for the nucleus, T the temperature, k_B the Boltzmann constant, and $\hbar$ the Planck constant. Even at a strong magnetic field of 1.5 T the thermal equilibrium polarization P is very low of 5×10^{-6} for ^{1}H, and 1×10^{-6} for ^{13}C (at body temperature). This means that only one of a million nuclei enables to be measured by standard clinical MRI scanner. The thermal polarization can be increased proportionally to the increasing magnetic field, and therefore the strength of the NMR signal also increases [90]. According to this fact 3 T MRI instruments have been introduced for clinical whole body imaging [91]. However, instruments with higher magnetic field face issues such as higher costs, radiofrequency penetration depths, and tissue contrast, and they increase dramatically with increasing field.

Until recent times the tissue anatomy imaging has been the most common application of magnetic resonance (MR) in medicine, however, one of the great strengths of MR is spectroscopy that allows imaging of tissue biochemistry. This phenomenon was realized already in the early MR applications in biological systems [92]. Although nowadays magnetic resonance imaging (MRI) has become a routine clinical tool, magnetic resonance spectroscopy (MRS) used in patients has lagged far behind. This was caused primarily due to low sensitivity of the measurement resulting in long measurement times and poor image resolution [93, 94, 95, 96]. In spite of this, ^{1}H-MRS measurements of cellular metabolites in a variety of tumor types have been shown to provide a sensitive means to diagnose disease and detect response.

2.1   MRI HARDWARE

A modern common MRI scanner (see Fig. 7) consists of three main components: (a) superconducting magnet, (b) radio-frequency (RF) system, and (c) gradient system. The function of the superconducting magnet is to create a strong static magnetic field B_0, however, to be able to have such a strong magnetic field the superconducting coil must be submerged into the liquid helium (lHe) at temperature of ~4.2 K and pressure of 1 atm. Thanks to these low temperatures one can achieve magnetic fields up to 7 T in commercially available systems, depending on the application.
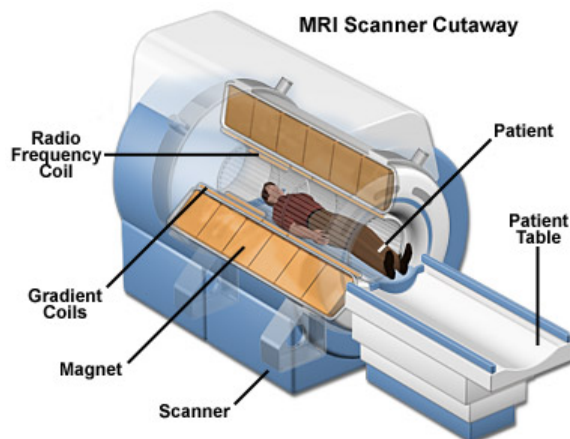
Figure 7: Simplified cutaway of today's typical MRI scanner for whole body medical application [97].

The RF system's function is to excite and detect the signal. It consists of transmitter, receiver and a coil. Suitably shaped pulses are generated and amplified by the transmitter, which then drives the coil. The coil creates an oscillating magnetic field that excites the spin system.

To encode the spatial information, the gradient coils create a magnetic field gradient. The precision of the transverse magnetization causes a time–varying magnetic field that induces a small oscillating electric current in a receiver coil. This allows measuring the free induction decay (FID) signal.
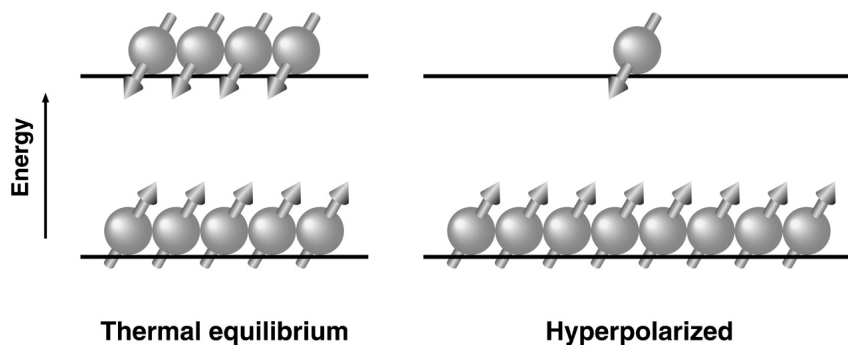
Figure 8: Pictorial description of the orientation of the nuclei at thermal equilibrium and in the hyperpolarized state. In the figure, the magnetic field (B_o) is directed vertically upwards [98].

2.2 HYPERPOLARIZATION

A conceptually opposite method to increase the NMR signal is to create an artificial, non-equilibrium distribution of the nuclei, or so called the "hyperpolarized" state. The difference between parallel ($N_{+\frac{1}{2}}$) or anti-parallel ($N_{-\frac{1}{2}}$) is increased by several orders of magnitude compared with the thermal equilibrium. This state is very nicely graphically described in the Figure 8: Hyperpolarized. There have been several methods developed, how could one increase the NMR signal using the "hyperpolarized" state: the "brute force" approach, parahydrogen-induced polarization, optical pumping methods, and dynamic nuclear polarization.

2.2.1 *The "brute force" polarization*

As described before thermal equilibrium polarization increases with increasing magnetic field strength, however, Equation 2 also defines that thermal equilibrium polarization rises with decreasing temperature. When the candidate molecule is inserted into an environment with very strong magnetic field at temperature close to 0 K, the polarization is increased by a factor of 10^3-fold. If the sample is then rapidly brought to 1.5 T and 310 K (i.e. without losses of polarization), it is therefore hyperpolarized at body temperature [98].

Even though the basic idea of the method sounds simple, to obtain a polarization level, where the hyperpolarized signal overtakes the ^{1}H signal of nowadays commonly used MRI, the temperature required for the "brute force" method would need to be just mK above absolute zero. Production of hyperpolarized noble gases such as ^{3}He and ^{129}Xe in large scale has been proposed, however, due to the technical challenges and high costs the "brute force" method has not yet been used for any *in vivo* experiments [99].

2.2.2   *Parahydrogen-induced polarization*

Parahydrogen-induced polarization (PHIP) method is based on the chemical reaction of the substrate molecule with parahydrogen. A parahydrogen is a state of hydrogen where its nuclei are oriented in such a way that their magnetic moments cancel. During this chemical reaction a substrate molecule containing ¹³C is hydrogenated with parahydrogen. The spin order of the parahydrogen molecule is converted to nuclear polarization of the ¹³C nucleus via a diabatic field cycling scheme [100].

PHIP method has been successfully applied for angiography measurements and for measuring tissue perfusion. Unfortunately until now the application to biological metabolites has been limited [101], even though the instrumentation that is required for PHIP is relatively simple. The limiting step in successful further development of PHIP is the catalyst development and hydrogenation chemistry, which are technically very challenging [89].

2.2.3   *Optical pumping method*

The optical pumping method is based on observation of transfer of the angular momentum from the electron spins of optically pumped Rb atoms to the nuclear spins of ³He or ¹²⁹Xe by spin-exchange collisions [102, 103]. In the magnetic field the light from the circularly polarized laser drives the electronic transition $S_{\frac{1}{2}}$-$P_{\frac{1}{2}}$ of the Rb atoms to selectively pump the ground-state Rb electrons entirely to the $+\frac{1}{2}$ (or $-\frac{1}{2}$) state. The optically pumped Rb atoms can transfer its electronic polarization to the nuclei of ³He or ¹²⁹Xe atoms via binary collisions, or via formation of loosely bound van der Waals molecules [104, 105]. Although the theory of hyperpolarization of noble gases by optical pumping method was discovered in the early 1960s, the recent progress in the development of high-power lasers allowed large-scale studies only recently [98, 106].

2.2.4   *Dynamic Nuclear Polarization*

Dynamic Nuclear Polarization (DNP) is based on a class of spin physics that was first described by an American physicist Albert W. Overhauser in the 1953. In his article he wrote: *"It is shown that if the electron spin resonance of the conduction electrons is saturated, the nuclei will be polarized to the same degree they would be if their gyromagnetic ratio were that of the electron spin."* In other words Overhauser proposed an idea that saturating the electron spin system would dramatically polarize the nuclear spins [107]. His theoretical hypotheses were experimentally demonstrated in the same year by Carver and Slichter [108].

DNP uses the approach of the transfer of high electron spin polarization to the nuclear spins in solid state. At temperatures close to absolute zero (~1 K), which can be achieved using liquid helium (lHe) at low pressure, the electron spin polarization posses a much higher polarization than ¹H or ¹³C, and approaches up to 100%

(Fig. 9.1). This is due to the different gyromagnetic ratio of electrons, which is 660 times larger compared to protons and even 2600 times larger compared to ^{13}C.

The unpaired free electron pool is generally provided by an organic free radical, although metal ions have also been used successfully [109]. The choice of radical depends on several factors including the solubility in the solution of interest, and the electron paramagnetic resonance (EPR) spectrum of the radical, which should have a line width that exceeds the Larmor frequency of the nuclear spin. Generally, radicals that fit these criteria are either nitroxides or trityls; the trityl OX063 is nowadays the most commonly used and the optimal concentration, for the speed of development and the level of polarization achieved, is ~15 mM, although this can vary between metabolites [110].

The electron spin polarization can be partially transferred to the nuclear spins using microwave irradiation (Fig. 9.2). The efficiency of this transfer depends on several factors, including the microwave frequency and power. The nuclear-spin polarization of ^{1}H and ^{13}C can be increased to 100% and 50%, respectively [111, 112].

To increase the signal MRI Gadolinium–based contrast agents such as Gadoteric acid (Dotarem®), or Gadoteridol (ProHance®) are usually also added to the sample before hyperpolarization. It has been reported that the addition of small quantities of Gd^{3+} substantially increases the hyperpolarization using the DNP technique with the trityl radical [113].

MRI contrast agents alter the relaxation times of atoms within body tissues where they are present after oral or intravenous administration. In MRI scanners sections of the body are exposed to a very strong magnetic field, a radiofrequency pulse is applied causing some atoms (including those in contrast agents) to spin and then relax after the pulse stops. This relaxation emits energy, which is detected by the scanner and is mathematically converted into an image. The MRI image can be weighted in different ways giving a higher or lower signal.

If a ^{13}C sample is now doped with free electrons by mixing it with a radical, the electron polarization can be partially transferred to the nuclei by continuous irradiation with microwaves near the electron resonance frequency (about 94 GHz at 3.35 T). Recently, the technique has been adapted allowing it to be applied to liquid-state ^{13}C MRS to produce a large (>10,000-fold) increase in sensitivity [89].

2.2.4.1   *Requirements for successful in vivo DNP*

Although there are many potential molecules that would be very interesting to study using DNP, very few fulfill the numerous criteria required for successful detection of their metabolism *in vivo*. A good candidate for hyperpolarization must at first have a long longitudinal relaxation time (T_1) of the labeled carbon in the liquid state. It needs to be transported and metabolized very rapidly within approximately five times its T_1 (1 – 3 min), and the labeled hyperpolarized molecule should probe an enzymatic reaction of biological significance, or one that can act as a reporter for cellular function. Its final product must be non-toxic, and the chemical shift difference between the resonances from the ^{13}C-labeled substrate and its metabolites
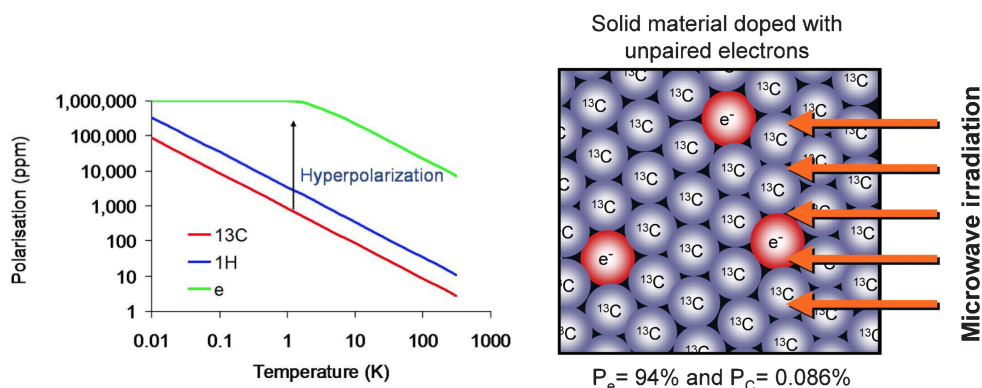
9.1: Thermal polarization of electrons, protons, and ¹³C atoms in the magnetic fields of the DNP polarizer.

9.2: Polarization transfer from the electrons of the doping material to the ¹³C atoms of candidate molecule by means of microwave irradiation.

Figure 9: Process of the polarization transfer during DNP from the electrons of the doping material (trityl radical) to ¹³C atoms of candidate molecule e. g. [5-¹³C]-L-glutamine [114, 98].

must be significantly large to enable easy recognition during *in vivo* measurements. To achieve a high degree of polarization, first, in the solid-state, the ¹³C-labeled metabolite must form a glass or amorphous solid lattice that allows the radical to be homogenously distributed; glass-formers such as glycerol, dimethyl sulfoxide (DMSO), or ethanol can be added to the sample to prevent crystallization. The dissolution process results in a substantial dilution of the polarized substrate before the intravenous injection. For successful DNP imaging following the injection, the hyperpolarized ¹³C-labelled molecule will be diluted by approximately two orders of magnitude before reaching the target tissue. Therefore a further requirement is that the candidate molecule has relatively high solubility (enabling concentration of 50 – 100 mM) to allow its polarization at high concentration. These limitations mean that relatively few metabolites fulfill all the criteria necessary for successful imaging *in vivo* following DNP, and even when a suitable molecule is found developing a working protocol for hyperpolarization can be technically challenging [89, 115, 116].

From these few metabolites several were already successfully hyperpolarized enabling fundamental biological processes to be probed. The most studied molecule is [1-¹³C]pyruvate, which was polarized up to 40% at 3.35 T and up to 64% at 4.64 T. It does not need any glassing solvent due to the fact that it produces amorphous glass by it self when frozen. On other molecules several scientific groups from all over the world are already working, namely on [1-¹³C]ethyl pyruvate, [1-¹³C]lactate, ¹³C-bicarbonate, [1,4-¹³C₂]fumarate, [2-¹³C]Fructose, [1-¹³C]ketoisocaproate, [1-¹³C]glutamate, and [1-¹³C]urea.[1]

---

1 For further references please see Brindle et al.(2011)[115]

2.2.4.2 *Hyperpolarization of glutamine*

Glutamine allows two possible isotope candidates that fulfill the requirements for successful DNP and following *in vivo* measurement: [1-^{13}C]glutamine and [5-^{13}C]glutamine (Fig. 10). The glutamine with ^{13}C nucleus at the C-1 position has significantly longer T_1 (24.6 s), compared to 16.1 s of glutamine with ^{13}C at C-5 position; however, the chemical shift change when glutamine is converted to glutamate is much smaller at the C-1 position (0.5 ppm) compared to 3.4 ppm for C-5 position. Despite the shorter T_1, which means that the polarization is much shorter-lived at this position, the larger chemical shift change means that [5-^{13}C]-L-glutamine is a more suitable substrate for detecting glutaminase activity than the C-1-labeled compound [116].
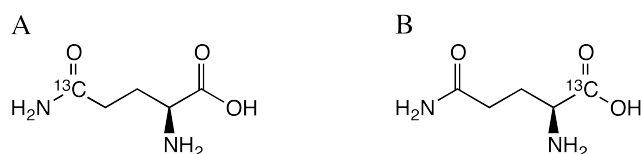
Figure 10: Suitable ^{13}C isotopes of L-glutamine for hyperpolarization using DNP:
(A) [5-^{13}C]-L-glutamine **(B)** [1-^{13}C]glutamine.

Elevated glutamine metabolism is postulated to be a marker of tumor growth and cell proliferation. For example, altered glutamine metabolism might be used to help identify hepatocellular carcinoma (HCC) within a cirrhotic liver [73] or identify malignant from benign disease when repeated biopsies are not possible. Glutamine is also already safely administered to patients [115].

HCC is the fifth most common malignancy worldwide and the third most common cause of cancer-related death. Radiologically, it can be difficult to identify a small HCC in the presence of a cirrhotic liver given the abnormal underlying tissue architecture. However, the metabolic differences between tumor and normal tissue may prove to be more useful in the detection of HCC. For example, the rate of glutamine uptake and metabolism to glutamate in HCC cells is up to 30-fold higher than in normal healthy hepatocytes, in part because of expression of a distinct membrane transporters [12, 73, 84, 116]. The recent study showed that glutamine could be polarized up to 5% [116]. Detection of abnormal metabolic fluxes or the accumulation of unusual metabolites could be used to monitor the predisposition to cancer in humans [88, 89]. Imaging can not only support an initial diagnosis but also monitor progress in terms of staging, restaging, treatment response, and identification of reoccurrence, both at the primary tumor and at distant metastatic sites [88].

AIMS OF THE THESIS

- Until now no preparation technique of ¹³C glutamine designed especially for *in vivo* ¹³C-MMR experiments was published. The first aim of the thesis was to prepare and optimize the preparation process for the hyperpolarization of the [5-¹³C]-L-glutamine using Dynamic Nuclear Polarization (DNP) for further for *in vivo* experiments using MRS measurement.

- If aim number one was successfully finished, the second aim of the thesis was to use the established sample preparation protocol, and measure the enzymatic conversion of the [5-¹³C]-L-glutamine to [5-¹³C]glutamate using glutaminase and cell cultures *in vitro* experiments with hyperpolarized ¹³C -glutamine.

Part II

MATERIALS AND METHODS

*Insanity: doing the same thing over and over
again and expecting different results.*

Albert Einstein

MATERIALS AND METHODS

4.1 HARDWARE

All the experiments were performed using the the HyperSense™ DNP polarizer (Oxford Instruments, Abingdon, UK) and the GE Signa® EXCITE™ 3.0 T MRI scanner (GE Healthcare, Milwaukee, USA) both located at GE Global Research center (GEGR) in Garching bei München, Germany, and on Bruker AVANCE 600 named "Laurel" located at Bavarian NMR Center (BNMRZ), Garching bei München, Germany.

4.1.1 *Hyperpolarizer*

The HyperSense™ DNP polarizer was used to polarize the ^{13}C atoms. It generally consists of three parts: 3.35 T superconducting magnet, 94 GHz solid–state microwave oscillator, and a variable temperature insert (VTI). The superconducting magnet is actively shielded and operates at temperature of 4.2 K because it is submerged in liquid helium (lHe), in a dewar vessel with supplementary cooling by liquid nitrogen (lN$_2$) in a concentric vessel around the He/coil container. The VTI holds the sample when it is inserted, and after sample insertion the VTI including the sample is submerged into lHe. The VTI is directly connected to the lHe reservoir via a capillary and the amount of lHe is regulated by a needle valve. The temperature at the VTI during the polarization process is set at 1.4 – 3.9 K using the change in the pressure.

During polarization the container with the sample is submerged in the lHe and the microwaves from the 94 GHz solid–state microwave oscillator are applied to transfer the hyperpolarization form the molecule with free electron (trytil, nitrooxide) to the candidate molecule. Depending on the molecular structure of the molecule the polarization time takes between 15 minutes and 4 hours. During the polarization the DNP polarizer measures constantly the solid-state polarization. The polarization increases in logatitmic way.

After the ^{13}C-compound is polarized to its maximum it needs to be dissolved and warmed up to the body temperature (37°C). Before the dissolution process the dissolution agent (~ 5 mL) is loaded into the specialized compartment. During the dissolution process the VTI including the sample container is taken out from the lHe and a dissolution agent, located in the separated compartment, is heated up to ~100°C at 10 bar. The dissolution wand is docked to the sample container and the heated dissolution agent is pushed into the cup containing the frozen sample by the inert helium gas. The sample is immediately dissolved and flushed out through a flexible hose into a collection flask, from where ~2 mL are injected into anNMR tube and immediately transported into the MRI scanner.
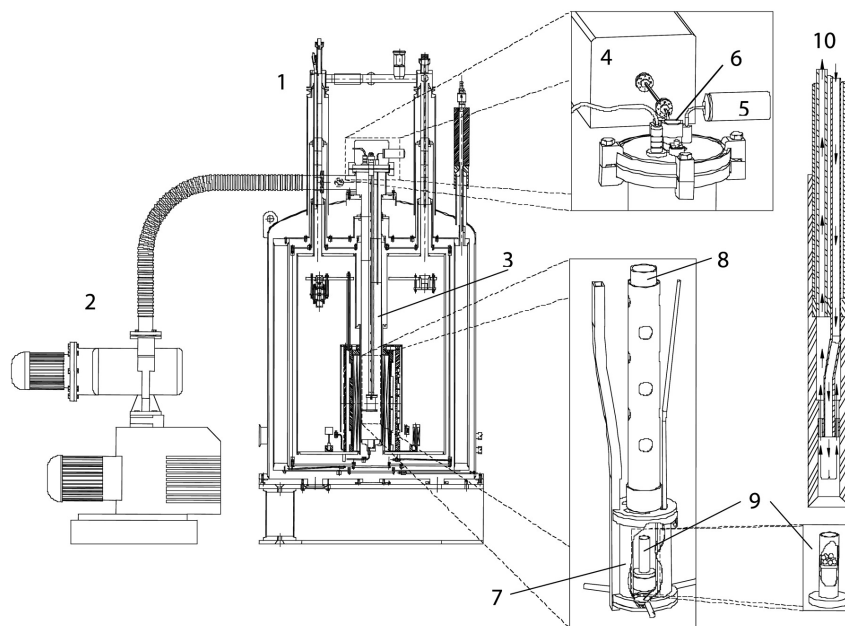
Figure 11: Schematic drawing of the DNP polarizer and parts. 1) DNP polarizer; 2) vacuum pump; 3) VTI; 4) microwave source; 5) pressure transducer; 6) sample port; 7) microwave container; 8) sample holder; 9) sample container; 10) dissolution wand. [110]

The routine maintenance of the HyperSense™ DNP polarizer consists mostly of refilling of the cryogens. The consumption of the lHe is ~2 L per single dissolution, whereas the lN$_2$ must be refilled approximately every two weeks.

4.1.2   *MRI scanner*

The GE Signa® EXCITE™ 3.0 T MRI scanner is a whole body type MRI scanner. This type is used daily in many hospitals all around the world. The magnet is ~200 cm long with a bore diameter of 60 cm with the highest levels of magnetic field homogeneity. Its whole body gradient coil has a maximum gradient amplitude of 23 mT/m and a maximum slew rate of 78 Tm^{-1}s^{-1}. Additionally a zoom gradient coil with 40 mT/m maximum gradient amplitude and 170 Tm^{-1}s^{-1} maximum slew rate is installed. The MRI scanner is controlled by GE software based on a Linux running based workstation.

For our experiments NMR tubes ($\varnothing$=8 mm) containing the sample were inserted into the custom-built solenoid coil surrounded by a heating module containing circulating warm water (adapted from patient warming system; Gaymar Industries, Orchard Park, NY). The temperature of the cell suspension can be adjusted and remained stable during the experiment. In order to improve the T$_2$* linewidth, susceptibility-matched plugs and NMR tubes (Doty Scientific, Columbia, SC, USA) were used. The solenoid transmit-receive ^{13}C coil was designed and optimized for 2 mL

Figure 12: The hardware equipment at GE Global Research centre in Garching bei München used for the experiment. 1) Oxford Instruments HyperSense™ DNP polarizer. 2) The GE Signa® EXCITE™ 3.0 T MRI scanner. 3) Brucker AVANCE III 600 "Laurel" located at Bavarian NMR Center (BNMRZ)

sample volume. The coil has 11 mm in diameter and 50 mm in length and is made of 9 turns of copper wire (∅=1.5 mm).

4.2 MRI MEASUREMENT PROTOCOL

After the dissolution ~2 mL of the sample were transferred from the collection flask into NMR tube (∅=8 mm), which was immediately transported into the coil located in the bore of the MRI scanner. The sample was first analyzed using the MRI scanner for its hyperpolarization using a sequence of hard pulses applied every 1 second in 128 cycles (~2 minutes) with a flip angle $\theta_{hp} = 10°$. Later to improve the signal a MRI contrast agent Gadoteridol (ProHance®) was added to the sample (40 μL/mL of sample) and thermal polarization was measured with a flip angle $\theta_{th} = 90°$ and hard pulses applied every 1 second for 4096 cycles (~68 min), respective 2048 cycles (~34 min). The hyperpolarization was than calculated from the acquired spectra using the following equation:

$$P_{hp}\,[\%] = P_{th}\frac{A_{hp}}{A_{th}}\frac{\sin(\theta_{th})}{\sin(\theta_{hp})} \qquad (3)$$

where P_{hp} represents the hyperpolarization, P_{th} is the thermal polarization, A_{hp} and A_{th} is amplitude at t=0, and θ is the flip angle applied during the hyperpolarization measurement (θ_{hp}), and during the thermal measurement (θ_{th}). The T_1 values were obtained by fitting of hyperpolarized NMR signal decay to Equation 4 that also includes the effect of radiofrequency (RF) pulsing with a given flip angle θ_{hp}=10°:

$$M_z(t) = M_0\sin\theta_{hp}(\cos\theta_{hp})^{t/TR}\exp(-t/T_1) \qquad (4)$$

where TR stands for the repetition time, M_o means the original magnetization before the RF pulse was applied and M_z is the magnetization after. θ_{hp} is the flip angle applied during the hyperpolarization measurement and t represents time.

4.3 SAMPLE PREPARATION

As already described in Section 2.2.4 glutamine (Gln) must fulfill several requirements to enable its polarization using the DNP method. During the preparation of the sample the following three items are important:

1. High solubility of the molecule while maintaining chemical stability, so that the injectable dissolution is sufficiently concentrated (enabling concentration of 50 – 100 mM).

2. The solution composition has to be chosen such that it forms an amorphous glass in the solid state.

3. All of the chemicals used need to be non–toxic for *in vivo* experiments [89, 115].

There are several limiting factors, which need to be taken into account during the preparation of Gln for DNP. Glutamine is normally available in a solid state in form of a white powder and as a molecule it has relatively low solubility in water (36.0 g/L at 18°C, 42.5 g/L at 25°C, and 48.0 g/L at 30°C), and therefore does not really fulfill the first requirement. Due to the fact that the optimal polarized volume in the HyperSense™ DNP polarizer is ~100 μL, and the final concentration during the injection for sufficient signal during *in vivo* measurement is 50 – 100 mmol/L, one has to design a process where solid glutamine is dissolved in the concentration of 2.5 – 5 mol/L (367.85 – 735.7 g/L) before hyperpolarization (before it is diluted by the dissolution agent to final concentration of 50 – 100 mmol/L).

The initial approach model in the preparation of [5-^{13}C]-L-glutamine for DNP was taken from Gallagher et al. (2008) [116], which describes the sample preparation as follows:

> L-glutamine (2.9 mg of [5-^{13}C]-L-glutamine; Sigma-Aldrich, UK) was added to 200 μL of glycerol and water (60:40 v/v) containing 15 mM of a trityl radical (GE-Healthcare, UK), giving a concentration of 100 mM. The sample was heated to 90°C for 15 min and then 10 μL aliquots were pipetted into liquid nitrogen. The resulting pellets were transferred to a precooled cup, which was screwed into a polytetrafluoroethylene (PTFE) tube and then quickly lowered into the center of the hyperpolarizer. The hyperpolarized sample was dissolved using 4 mL of solution of phosphate-buffered saline (137 mM NaCl, 10 mM phosphate buffer, 2.7 mM KCl, pH 7.4; Sigma-Aldrich, UK) and 100 mg/L ethylenediaminetetraacetic acid (EDTA; Sigma-Aldrich, UK) at 180°C giving a final glutamine concentration of 2.5 mM.

Even though this procedure is elegant and relatively simple to proceed, one limiting factor was given to follow this preparation – final concentration. As described

previously one of the requirement for successful *in vivo* experiments is the final glu-
tamine concentration of 50 – 100 mM before injection. Preparation by Gallagher et
al. did not have to fulfill this requirement since the study did not include *in vivo*
experiments, and therefore the final concentration is 20 times smaller (2.5 mM). For
successful *in vivo* experiments the preparation technique must have been modified
to enable higher concentration.

4.3.1 *L-glutamine solubility in glassing agents*

The first approach was to study the solubility of L-glutamine (Gln) in different glass-
ing solvents. The suitable glassing solvent tested were glycerol, ethanol, propan-1,2-
diol, and their mixtures with water (50:50 v/v). First, the glycerol was tested as
a candidate for the glassing agent. Different amounts of L-glutamine in range of
0.25 – 0.50 mmol (0.25, 0.28, 0.31, 0.34, 0.37, 0.40, 0.43, 0.46, 0.48, 0.50 mmol) were
added to 100 μL of glycerol and the samples were submerged into ultrasonic bath
at 25°C, and every 10 minutes for the next 1 hour, all samples were checked if Gln
is dissolved completely, and if not mixed using a vortex mixer for several seconds.
This procedure was repeated with other cadidate molecules for the galssing agents:
ethanol, propan-1,2-diol, and mixtures of glycerol, ethanol, propan-1,2-diol with H_2O
(50:50 v/v).

4.3.2 *L-glutamine solubility under basic conditions*

Due to the fact that the glutamine solubility in H_2O is 36 g/L, it was no surprise
that none of the glassing solvent was able to dissolve Gln completely. However, the
solubility of L-glutamine and other zwitterionic amino acids can be improved by
adding a base such as sodium hydroxide (NaOH) or potassium carbonate (K_2CO_3)
that would produce glutamine aqueous anionic species (Fig. 13).
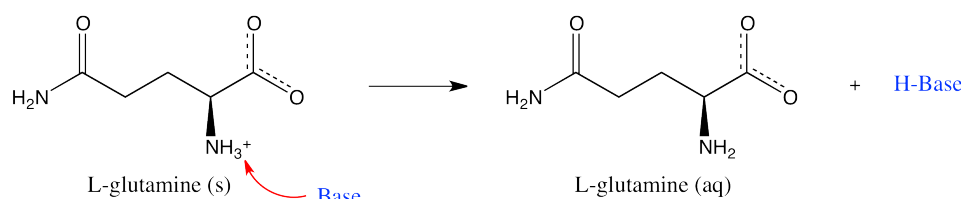
Figure 13: Reaction of glutamine zwitterion with base.

4.3.2.1 *Sodium hydroxide (NaOH) as a base*

The acid dissociation constant (pK_a) of the Gln amino group is 9.13, therefore a
strong base such as sodium hydroxide (NaOH) was chosen to be tested first. The
experiment was designed so that the theoretical concentration of L-glutamine after
dissolution (~5 mL) would be 50 mmol/L or 100 mmol/L, respectively. The exact
sample preparation was following:

> L-glutamine (0.25 mmol or 0.50 mmol; Sigma-Aldrich, S.Louis, MO, USA) was dissolved in glycerol (100 μL; Sigma-Aldrich, S.Louis, MO, USA) with added 12M NaOH (5 - 50 μL in range of 5 μL (5, 10, 15, 20, 25, 30, 35, 40, 45, 50 μL); Sigma-Aldrich, S.Louis, MO, USA)

Therefore together 20 samples each with different amount of L-glutamine vs. sodium hydroxide were examined. In both cases the minimal concentration of sodium hydroxide required for complete dissolution of the L-glutamine within 60 minutes was examined.

4.3.2.2 *Potassium carbonate (K_2CO_3) as a base*

Due to the fact that sodium hydroxide (NaOH) also acts as a nucleophile and can hydrolyze amide groups, the non-nucleophilic base potassium carbonate (K_2CO_3) was tested as a possible candidate for a base in the preparation protocol for furthe *in vivo* experiments. The aim was to find out how much of K_2CO_3 is required to dissolve 0.25 mmol of Gln in 100 μL of glycerol within 60 minutes. The maximal concentration of K_2CO_3 in H_2O) is 8.09 mol/L, and therefore the amount of K_2CO_3 added to the examined sample was increased to $15 - 60$ μL compared to previous experiment. The exact sample preparation was following:

> L-glutamine (0.25 mmol; Sigma-Aldrich, S.Louis, MO, USA) was dissolved in glycerol (100 μL; Sigma-Aldrich, S.Louis, MO, USA) with added 8.09M K_2CO_3 (15 - 60 μL in range of 5 μL (15, 20, 25, 30, 35, 40, 45, 50, 55, 60 μL); Sigma-Aldrich, S.Louis, MO, USA)

The best performing preparation mixture using 8.09M K_2CO_3 was prepared using [5-^{13}C]glutamine (Sigma-Aldrich, S.Louis, MO, USA) and dissolved in 2 mL of D_2O and analyzed using the 14.1 T NMR spectrometer.

The hyperpolarization measurement was also examined. To the [5-^{13}C]glutamine (Sigma-Aldrich, S.Louis, MO, USA) mixture dissolved using potassium carbonate, trytil radical (OX063, 55 μmol; GE Healthcare, Milwaukee, WI, USA) and GdDOTA complex (Dotarem®) (7 μmol; Guerbet, Roissy, France) was added and hyperpolarized with Hypersense™ 3.35 T Dynamic nuclear polarizer (DNP) (Oxford Instrument, Abingdon, UK) for ~1h at 94.105 GHz. The solid samples were rapidly dissolved with TRIS (5 mL, 30mM) buffered H_2O and the liquid state polarization was measured according to MRI measurement protocol described in Section 4.2.

4.3.3 *L-glutamine solubility under acidic conditions*

Acidic conditions of the solution can also increase the solubility of glutamine (Gln). The hydronium ion (H_3O^+) can provide a proton to the molecule of glutamine thus forming a aqueous cationic species. As a source of H_3O^+ ions a hydrochloric acid

(HCl) was used. First 0.25 mmol of L-glutamine were examined to be dissolved using different amounts of 12M HCl (5 – 50 μL).

> L-glutamine (0.25 mmol; Sigma-Aldrich, S.Louis, MO, USA) was dissolved in glycerol (100 μL; Sigma-Aldrich, S.Louis, MO, USA) with added 12M HCl (5 - 50 μL in range of 5 μL (5, 10, 15, 20, 25, 30, 35, 40, 45, 50 μL); Sigma-Aldrich, S.Louis, MO, USA)

Due to the fact no concentration of HCl was able to dissolve 0.25 mmol of L-glutamine completely, the experiment was inverted and the maximum amount of L-glutamine able to be dissolved by 25 μL of 12M HCl was determined.

> L-glutamine (0.05 – 0.24 mmol in range of 2 mmol (0.05, 0.07, 0.10, 0.12, 0.14, 0,16, 0.18, 0.20, 0.22, 0.24 mmol); Sigma-Aldrich, S.Louis, MO, USA) was dissolved in glycerol (100 μL; Sigma-Aldrich, S.Louis, MO, USA) with added 25 μL of 12M HCl(Sigma-Aldrich, S.Louis, MO, USA)

The best performing preparation mixture using 12M HCl was prepared using [5-^{13}C]glutamine (Sigma-Aldrich, S.Louis, MO, USA), and then dissolved in 2 mL of D$_2$O and analyzed using the 14.1 T NMR spectrometer.

4.3.4   *Influence of temperature on L-glutamine's solubility*

The second physical property next to the pH, which increases the solubility of glutamine in glassing solvents, is temperature. However, as described in Section 1.1.2 glutamine is not very stable in aqueous form and very likely undergoes a reaction to pyroglutamic acid (pGlu), when the temperature is increased. As measured by Arii et al. the degradation in higher temperature is not very fast and highly depends on the pH of the buffered solution [20]. In Figure 2.2 degradation of the glutamine is described at 70°C. From the measurements one can see that even at very high pH (9.31, 11.01) the degradation of 20% of glutamine takes several hours. With this knowledge experiments of finding the minimum amount of 12M NaOH able to dissolve Gln completely (giving final concentration 50 mmol/L and 100 mmol/L), were repeated at 70°C. The detailed procedure is the same as described in Section 4.3.2.1, however using ultrasonic bath at 70°C. For better understanding it is described in following box:

> L-glutamine (0.25 mmol or 0.50 mmol; Sigma-Aldrich, S.Louis, MO, USA) was dissolved in glycerol (100 μL; Sigma-Aldrich, S.Louis, MO, USA) with added 12M NaOH (5 - 50 μL in range of 5 μL (5, 10, 15, 20, 25, 30, 35, 40, 45, 50 μL); Sigma-Aldrich, S.Louis, MO, USA) under 70°C.

4.3.5 *Influence of pH and temperature on glutamine's stability*

From the literature described in Section 1.1 we know that glutamine is labile in aqueous solution. The increased base content and increased temperature enhances the glutamine's solubility, however, it can also increase the chance of glutamine to undergo a unwanted reaction to glutamic acid (Glu) and pyroglutamic acid (pGlu). The aim of the following experiment was to find out how well the [5-^{13}C]-L-glutamine undergoes the reaction to Glu and pGlu in different conditions.

Four different scenarios of sample preparation were examined using the 14.1 T NMR scanner on the presence of side products of glutamic and pyroglutamic acids. First, the best performing preparation techniques from Section 4.3.2.1 giving the final concentration 50 mmol/L and 100 mmol/L were prepared at 30 °C with the following procedure:

The results are available in Section 5.4 on page 44.

> [5-^{13}C]-L-glutamine (0.25 mmol or 0.50 mmol; Sigma-Aldrich, S.Louis, MO, USA) was dissolved in glycerol (100 μL; Sigma-Aldrich, S.Louis, MO, USA) with added 12M NaOH (20 μL or 35 μL; Sigma-Aldrich, S.Louis, MO, USA) at 30°C. When Gln was completely dissolved (after 50 – 60 min) the sample was diluted in 2 mL D$_2$O and examined using 14.1 T NMR scanner.

Second, the effect of temperature during the preparation was examined on the presence of side products of glutamic and pyroglutamic acids using the 14.1 T NMR scanner. The best performing preparation techniques from Section 4.3.4 giving the final concentration 50 mmol/L and 100 mmol/L were prepared at 30 °C with the following preparation:

The resulted spectra are available in Figure 16 on page 45.

> [5-^{13}C]-L-glutamine (0.25 mmol or 0.50 mmol; Sigma-Aldrich, S.Louis, MO, USA) was dissolved in glycerol (100 μL; Sigma-Aldrich, S.Louis, MO, USA) with added 12M NaOH (25 μL or 45 μL; Sigma-Aldrich, S.Louis, MO, USA) at 70°C. When Gln was completely dissolved (after 50 – 55 min) the sample was diluted in 2 mL D$_2$O and examined using 14.1 T NMR scanner.

4.3.6 *Increasing the viscosity of the sample to suppress the side reactions*

During the sample preparations procedure side products such as glutamic acid (Glu) and pyroglutamic acid (pGlu) might occur when the NaOH concentration or temperature was increased. As described in Section 1.1.1 and 1.1.2 glutamine is not very stable in aqueous form and very likely undergoes a reaction to Glu and (pGlu). Due to this fact the sample preparation procedure was modified.

To decrease the side reaction rate an idea to use the viscosity of the glassing solvent as a potential "break" of the side reaction was examined. The idea behind the approach was that glycerol is very viscous solvent and its viscosity may slow down the side reactions, especially the reaction of glutamine to pyroglutamic acid. The

14.1: Trytil radical OX063   14.2: Gadoteric   acid   14.3: Gadoteridol
                              (Dotarem®)   (ProHance®)
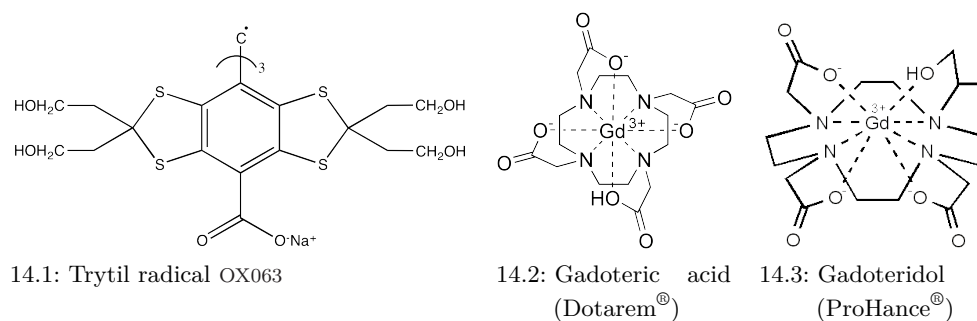
Figure 14: Chemical structures of chemicals used as an electron dopant in DNP experiments.

only possibility how to make glycerol even more viscous was to reduce the amount of water present in the sample during the preparation, therefore the concentration of the NaOH added was increased from the 12 mol/L to 27 mol/L, and thus the amount of H₂O was decreased.

First, the minimal concentration of sodium hydroxide (27M, NaOH) required for complete dissolution of the L-glutamine (0.50 mmol) within 60 minutes was examined. The detailed preparation procedure was following:

> L-glutamine (0.25 mmol or 0.50 mmol; Sigma-Aldrich, S.Louis, MO, USA) was dissolved in glycerol (100 μL; Sigma-Aldrich, S.Louis, MO, USA) with added 27M NaOH (5 - 50 μL in range of 5 μL (5, 10, 15, 20, 25, 30, 35, 40, 45, 50 μL); Sigma-Aldrich, S.Louis, MO, USA)

The best performing preparation mixture using 27M NaOH was prepared using [5-¹³C]glutamine (Sigma-Aldrich, S.Louis, MO, USA). To the sample OX063 radical (55 μmol; GE Healthcare, Milwaukee, WI, USA) and GdDOTA complex (Dotarem®) (7 μmol; Guerbet, Roissy, France) was added and hyperpolarized with Hypersense™ 3.35 T Dynamic nuclear polarizer (DNP) (Oxford Instrument, Abingdon, UK) for ~1h at 94.105 GHz. The solid samples were rapidly dissolved with TRIS (5 mL, 30mM) buffered H₂O and measurend using the MRI scanner according to MRI experiment protocol described in Section 4.2.

4.3.7 *Comparison of [5-¹³C]glutamine and L-glutamine hyperpolarization*

Due to the fact that the liquid-state polarization obtained compared to the solid-state polarization obtained was very low, actually in range of ppt and not percentages, a test comparing the hyperpolarization of [5-¹³C]-L-glutamine and L-glutamine was performed. The exact preparation process was following:

> [5-¹³C]-L-glutamine or L-glutamine (0.5 mmol; Sigma-Aldrich, S.Louis, MO, USA) was dissolved under 25°C in glycerol (100 μL; Sigma-Aldrich, S.Louis, MO, USA)

> with added NaOH (35 μL, 27M; Sigma-Aldrich, S.Louis, MO, USA). To the sample OX063 radical (55 μmol; GE Healthcare, Milwaukee, WI, USA) and GdDOTA complex (Dotarem®) (7 μmol; Guerbet, Roissy, France) was added and hyperpolarized with Hypersense™ 3.35 T Dynamic nuclear polarizer (DNP) (Oxford Instrument, Abingdon, UK) for ~1h at 94.105GHz. The frozen solid samples were rapidly dissolved with TRIS (5 mL, 30mM) buffered H_2O and the hyperpolarization was analyzed using 3.0 T MRI scanner (128 scans/repetition time 1 s). Later a Gadoteridol (ProHance®) was added to the sample (40 μL/mL of sample) and thermal polarization was measured using 3.0 T MRI scanner (4096 scans/repetition time 1 s).

4.3.8 *Metal analysis*

Due to the similar results in liquid-state polarization but large differences in solid-state polarization in previous experiments (see Section 4.3.7 and 5.7.2) a detailed metal analysis was performed. The presence of impurities such as ferromagnetic metals (e.g. Cu, Ni) can be the reason of fast relaxation of [5-^{13}C]-L-glutamine polarization in liquid state. These metals could have been used during the synthesis of [5-^{13}C]-L-glutamine as part of a catalysts. Their residue might have been still present in the sample even in very small amounts after the purification. The [5-^{13}C]-L-glutamine was therefore ordered from all available suppliers, which had [5-^{13}C]-L-glutamine on sale: a) Sigma-Aldrich Co. LLC (St. Louis, MO, USA); b) Cambridge Isotope Laboratories, Inc (Andover, MA, USA); c) Toronto Research Chemicals (Ontario, Canada). However, only Sigma-Aldrich Co. and Cambridge Isotope Laboratories were able to deliver their product. The obtained samples were analyzed by the Chemical and Structural Analysis Laboratory (GE Global Research, General Electric Company, Niskayuna, NY, USA) using the High Resolution Inductively Coupled Plasma Mass Spectrometry (HR-ICP-MS). The exact measuring procedure was following:

> For the HR-ICP-MS ~1 mg aliquots of each glutamine sample were weighed by difference onto Fisher brand weighing papers by microbalance and transferred into trace metal-free acid-pre-cleaned (3× H_2O rinse, followed by fill in 25% aqua regia + 10% HF and rinse 5× H_2O) 15mL natural-cap centrifuge tubes (VWR, Radnor, PA, USA). Samples were run in duplicate or triplicate as weight allows, with one sample reserved for sample-spike measurement. Samples were then brought into a class 100 clean room for digestion. Tubes were placed in the fume hood for the following reagent additions: 3 mL 33% Optima grade HNO_3 and 3 mL 33% Optima grade HCl. 0.2 mL of ~50 ppb stock Rh in 1% HCl was added to each sample to serve as an internal standard and samples were brought to a total volume of 10mL with H_2O. Three procedural blanks were carried throughout.

All standard and quality control intermediates as well as internal standard were prepared in Nalgene™ volumetric flasks or 50 mL natural-cap centrifuge tubes (VWR, Radnor, PA, USA) that had been pre-cleaned (rinsed 3× H_2O, filled with

25% aqua regia + 10% HF, rinsed 5× H₂O). Calibration standards: 1, 2, 5, 10, 20, 50, 100, 200 and 500 ppt, 1, 2, 5, 10, 20, 50 and 100 ppb Al, As, Ba, Be, Bi, B, Cd, Ca, Ce, Cs, Cr, Co, Cu, Dy, Er, Eu, Gd, Ga, Ho, In, Fe, La, Pb, Li, Lu, Mg, Mn, Nd, Ni, P, K, Pr, Re, Rb, Sm, Sc, Se, Na, Sr, Tb, Tl, Th, Tm, U, V, Yb, Y, Zn, Sb, Ge, Hf, Mo, Nb, Si, Ag, Ta, Te, Sn, Ti, W and Zr in 2% HNO₃/0.06% HF/0.06% HCl with 1ppb Rh used as an internal standard. Quality control intermediates: provides external calibration check for all elements of interest except Bi and In.

The [5-¹³C]-L-glutamine (Cambridge Isotope Laboratories Inc., Andover, MA, USA), which proved to have lesser amount of Cu and Ni was used for further hyperpolarization examination and compared to hyperpolarization spectra of [5-¹³C]-L-glutamine (Sigma-Aldrich Co. LLC, St. Louis, MO, USA). The following procedure was used:

The resulted spectra are available in Figure 22 on page 51.

> [5-¹³C]-L-glutamine (0.5 mmol; Cambridge Isotope Laboratories Inc., Andover, MA, USA) was dissolved under 30°C in glycerol (100 μL; Sigma-Aldrich, S.Louis, MO, USA) with added NaOH (35 μL, 27M; Sigma-Aldrich, S.Louis, MO, USA). To the sample OX063 radical (55 μmol; GE Healthcare, Milwaukee, WI, USA) and GdDOTA complex (Dotarem®) (7 μmol; Guerbet, Roissy, France) was added and hyperpolarized with Hypersense™ 3.35 T Dynamic nuclear polarizer (DNP) (Oxford Instrument, Abingdon, UK) for ~1h at 94.105GHz. The frozen solid samples were rapidly dissolved with TRIS (5 mL, 30mM) buffered H₂O and the hyperpolarization was analyzed using 3.0 T MRI scanner (128 scans/repetition time 1 s). Later a Gadoteridol (ProHance®) was added to the sample (40 μL/mL of sample) and thermal polarization was measured using 3.0 T MRI scanner (4096 scans/repetition time 1 s).

4.3.9 *Loss of the signal due to the molecule's nature*

To prove that the lost of the signal is not due to any additional impurities and elements present in the sample but by the nature of the molecule it self, a test was designed where [5-¹³C]-L-glutamine was forced to undergo the reaction to glutamic acid completely. This was done using high concentration NaOH via the S$_N$2t mechanism described in Figure 17. Under same condition [5-¹³C]glutamic acid was also prepared. Due to the low solubility of glutamic acid (8.64 g/L at 25 °C) the amount of dissolved Gln and Glu must have been modified from the previous experiments. The exact sample preparation was following:

The resulted spectra are available in Figure 23 on page 54.

> [5-¹³C]-L-glutamine or [5-¹³C]glutamic acid (5.7 μmol; both Cambridge Isotope Laboratories Inc., Andover, MA, USA) was dissolved in glycerol (100 μL; Sigma-Aldrich, S.Louis, MO, USA) with added NaOH (60 μL, 27M; Sigma-Aldrich, S.Louis, MO, USA) completely in temperature conditions under 30°C. To the sample OX063 radical (55 μmol; GE Healthcare, Milwaukee, WI, USA) and GdDOTA complex (Dotarem®) (7 μmol; Guerbet, Roissy, France) was added and hyperpolarized with Hypersense™ 3.35 T Dynamic nuclear polarizer (DNP) (Oxford

Instrument, Abingdon, UK) for ~1h at 94.105GHz. The frozen solid samples were
rapidly dissolved with TRIS (5 mL, 30mM) buffered H_2O and the hyperpolariza-
tion was analyzed using 3.0 T MRI scanner (128 scans/128 s). Later a Gadoteridol
(ProHance®) was added to the sample (40 μL/mL of sample) and thermal polar-
ization was measured using 3.0 T MRI scanner (4096 scans/4096 s).

The obtained hyperpolarization spectra and polarization information were compared.

4.3.10   *Loss of the polarization due to relaxation through scalar coupling (type II)*

From the results of previous experiment (Section 5.7.3) we knew that the loss of the
[5-^{13}C]-L-glutamine hyperpolarization in liquid state is due to the molecule's natural
behaviour. In fact there are several mechanisms that contribute to the relaxation rate
(R_1) of ^{13}C nucleus: dipole–dipole interaction (R_1^d), paramagnetic relaxation rate
(R_1^{para}), chemical shift anisotropy (R_1^{csa}), scalar relaxation (R_1^{sc}), and spin-rotation
(R_1^{sr}) [117]. The relaxation rate (R_1) is a sum of these five terms according to:

$$R_1 = \frac{1}{T_1} = \sum R_1^d + R_1^{para} + R_1^{csa} + R_1^{sc} + R_1^{sr} \tag{5}$$

The dipole–dipole interaction (R_1^d) depends on the temperature via the variation
of the molecular correlation time, on the other hand paramagnetic relaxation rate
(R_1^{para}), chemical shift anisotropy (R_1^{csa}), and scalar relaxation (R_1^{sc}) are dependent
on the external magnetic field (B_0). The chemical shift anisotropy (R_1^{csa}) increases
at higher fields, whereas the paramagnetic relaxation rate (R_1^{para}) shows a marked
increase at lower fields (e. g. when nitroxide radicals such as TEMPO are used) [118].
The contribution of the scalar coupling relaxation can easily be related to the applied
field through the frequency difference term, as follows:

$$R_1^{sc} = \frac{8\pi^2 J^2}{3} I_X (I_X + 1) \frac{\tau_{sc}}{1 + (\omega_{^{13}C} - \omega_X)^2 \tau_{sc}^2} \tag{6}$$

where J represents the scalar coupling constant between ^{13}C and a spin X. The I_X
is to the spin quantum number of the coupled nucleus, τ_{sc} is the correlation time
characteristic of the scalar interaction, and $\omega_{^{13}C}$ and ω_X are the Larmor angular
frequencies of scalarly coupled nuclei [117, 119]. The scalar coupling interaction be-
tween the active nuclei, which determines the multiplicity of NMR signals, affects the
relaxation mechanism when the coupling constant is time-dependent. This occurs if
the coupling constant is modulated by the chemical exchange (i.e., type I scalar relax-
ation, when τ_{sc} is the inverse of the exchange rate) or if the spin state of the coupled
nucleus changes rapidly because of other relaxation mechanisms (i.e., type II scalar
relaxation, where τ_{sc} is the T_1 of a fast-relaxing nucleus, which is usually quadrupo-
lar). At a very low field, the Larmor frequencies become sufficiently equivalent so
that the type II contribution cannot be neglected leading to fast relaxation through
this mechanism. This can be demonstrated by applying Eq. 6 to the ^{13}C–^{14}N spin

system ($I_{14N} = 1$). We can assume that the $J_{13C-14N}$ is ~15 Hz, and the T_1 for ^{14}N is ~ 1×10^{-3} s. With given laboratory magnetic field averaged for the time spent by the sample in each point of the transfer path was about 650 μT the ω of ^{13}C and ^{14}N can be calculated using the following equation:

$$\omega_X = \gamma_X 2\pi B_0 10^6 \tag{7}$$

that means that ω_{13C} is 47037 rad/sec (10.7 MHz/T), and 13628 rad/sec=3.1 MHz/T for ω_{14N} With this knowledge we can calculate the R_1^{sc} using Equation 6:

$$R_1^{sc} = \frac{8\pi^2 J^2}{3} I_{14N}(I_{14N} + 1)\frac{T_{1,14N}}{1 + (\omega_{13C} - \omega_{14N})^2(T_{1,14N})^2} \tag{8}$$

$$R_1^{sc} = \frac{8\pi^2 15^2}{3} 1(1 + 1)\frac{1 \times 10^{-3}}{1 + (47037 - 13628)^2(1 \times 10^{-3})^2}$$

$$R_1^{sc} = 1.6 \ s^{-1}$$

To prove the hypotheses that type II relaxation through scalar coupling is the cause of the loss of the liquid state polarization observed experimentally, first, the magnetic field profile during transport needed to be characterized. The absolute value of the magnetic field vector along the travel path was measured using a Hall Gaussmeter (Model 455 DSP, Lake Shore Cryotronics Inc., Westerville, OH, USA). To proof the contribution of relaxation through scalar coupling is responsible for the fast signal decay four different experiments were performed. First, [5-^{13}C]-L-glutamine was transported with and without 0.2 T permanent magnet attached to the NMR tube during the transport from the polarizer to MRI scanner. To proof the coupling of ^{13}C on C-5 position and amide ^{14}N, the [5-^{13}C,^{15}N]-L-glutamine with ^{15}N in amide group was examined in the same way as [5-^{13}C]-L-glutamine – with and without 0.2 T permanent magnet from DNP polarizer to MRI scanner. The exact procedure of the experiment was the following:

The results are available in Section 5.7.4 on page 53.

[5-^{13}C]-L-glutamine (60 μmol; Cambridge Isotope Laboratories Inc., Andover, MA, USA) or [5-^{13}C, ^{15}N]glutamine (60 μmol; Toronto Research Chemicals, Toronto, ON, Canada) was dissolved in glycerol (100 μL; Sigma-Aldrich, S.Louis, MO, USA) with added NaOH (35 μL, 27M; Sigma-Aldrich, S.Louis, MO, USA) completely in temperature conditions under 30°C. To the sample OX063 radical (55 μmol; GE Healthcare, Milwaukee, WI, USA) and GdDOTA complex (Dotarem®) (7 μmol; Guerbet, Roissy, France) was added and hyperpolarized with Hypersense™ 3.35 T Dynamic nuclear polarizer (DNP) (Oxford Instrument, Abingdon, UK) for ~1h at 94.105GHz. The frozen solid samples were rapidly dissolved in 5 mL of 30 mM TRIS buffer and 1.3 mM EDTA in D₂O. The sample was transported from the DNP polarizer to MRI scanner either in Earth's magnetic field or 0.2 T permanent magnet was attached to sample containing NMR tube. The sample's polarization was analyzed using 3.0 T MRI scanner (128 scans, repetition time 1 s). Later 40 μL/mL of Gadoteridol (ProHance®) was added to the sample and thermal polarization was measured using 3.0 T MRI scanner (2048 scans, repetition time 1 s).

Part III

R E S U L T S

*A man came to this world
to be, work, and live.
Only wise tries to push our world further.
And only fool tries to stop him.*

— Jan Werich

RESULTS

5.1 L-GLUTAMINE SOLUBILITY IN GLASSING AGENTS

The first approach was to study the solubility of glutamine in different glassing solvents. The suitable glassing solvent tested were glycerol, ethanol, propan-1,2-diol, and their mixtures with water (50:50 v/v). Unfortunately none of the amount of glutamine (0.25 – 0.50 mmol) tested was able to be dissolved completely in either of the glassing solvent or their mixtures with water within 60 minutes.

5.2 L-GLUTAMINE SOLUBILITY UNDER BASIC CONDITIONS

Since glutamine did not dissolve in any of suitable glassing solvent under neutral conditions, the conditions had to be changed to either basic or acidic to improve the solubility of L-glutamine. For basic conditions in the glassing agent two bases were tested: sodium hydroxide (NaOH) and potassium carbonate (K_2CO_3).

5.2.1 *Sodium hydroxide as a base*

The aim of this test was to find out how much of 12M NaOH is required to dissolve 0.25 mmol of L-glutamine, respective 0.50 mmol, in 100 μL of glycerol. The amount of L-glutamine would give the final concentration during the injection of 50 mmol/L, respectively of 100 mmol/L in volume of 5 mL of injectable buffer solution during *in vivo* experiments. The results are summarized in Table 1 and Table 2.

The results showed that the minimum amount of sodium hydroxide (12M NaOH) required to dissolve 0.25 mmol of L-glutamine in 100 μL of glycerol within 60 minutes is 25 μL, and 45 μL to dissolve 0.50 mmol of L-glutamine. This means that to dissolve 0.25 mmol of L-glutamine completely 0.375 mmol of NaOH is required in the mixture of 100 μL of glycerol and 25 μL of water. To dissolve 0.50 mmol of glutamine within

NaOH (12M) [μL]	5	10	15	20	25	30	35	40	45	50
L-glutamine [mmol]	0.25	0.25	0.25	0.25	0.25	0.25	0.25	0.25	0.25	0.25
Glycerol [μL]	100	100	100	100	100	100	100	100	100	100
Dissolution time [min]	–	–	–	–	55	50	40	40	30	15

Table 1: Summary of the experiment results testing the L-glutamine (0.25 mmol) solubility at the presence of the strong base sodium hydroxide (12M NaOH) in 100 μL glycerol.

NaOH (12M) [μL]	5	10	15	20	25	30	35	40	45	50
L-glutamine [mmol]	0.50	0.50	0.50	0.50	0.50	0.50	0.50	0.50	0.50	0.50
Glycerol [μL]	100	100	100	100	100	100	100	100	100	100
Dissolution time [min]	–	–	–	–	–	–	–	–	60	55

Table 2: Summary of the experiment results testing the L-glutamine (0.50 mmol) solubility at the presence of the strong base sodium hydroxide (12M NaOH) in 100 μL glycerol.

60 minutes 0.675 mmol of sodium hydroxide is required in mixture of 100 μL glycerol and 45 μL H_2O.

It is clear that the amount of NaOH required increases with the increasing amount of L-glutamine, however, the dependence between the amount of NaOH and Gln was not linear. Less of the NaOH was needed in case of 0.50 mmol of glutamine dissolving. This was caused by the water added with the NaOH, and therefore increasing the overall sample volume (125 vs. 145 μL). This was demonstrated by an experiment, where L-glutamine (0.25 mmol) was completely dissolved in glycerol (100 μL) with added 7.5M NaOH (0.338 mmol, 45 μL) after 45 minutes (same time as in case of 0.50 mmol Gln), and therefore perfectly proofs the hypotheses.

5.2.2 *Potassium carbonate as a base*

Due to the fact that sodium hydroxide (NaOH) can also act as a nucleophile as shown in Figure 18, non-nucleophilic base potassium carbonate (K_2CO_3) was tested as a possible candidate for the replacement of NaOH in its role as a base. First, the aim was to find out how much of 8.09M K_2CO_3 (maximal concentration in H_2O) is required to dissolve 0.25 mmol of L-glutamine in 100 μL of glycerol within 60 minutes. The results are summarized in Table 3.

K_2CO_3 (8.09M) [μL]	15	20	25	30	35	40	45	50	55	60
L-glutamine [mmol]	0.25	0.25	0.25	0.25	0.25	0.25	0.25	0.25	0.25	0.25
Glycerol [μL]	100	100	100	100	100	100	100	100	100	100
Dissolution time [min]	–	–	–	–	–	–	–	–	60	55

Table 3: Summary of the results of the experiment testing the L-glutamine (0.25 mmol) solubility at the presence of the base potassium hydroxide (8.1M) in 100 μL glycerol.

Potassium carbonate (pK_a=10.3) is not such a strong base as sodium hydroxide (pK_a=13), and therefore the amount of K_2CO_3 required to dissolve 0.25 mmol of L-glutamine was higher compared to the experiment with NaOH (see Tab. 1 for reference). To dissolve 0.25 mmol of L-glutamine 55 μL of 8.09M K_2CO_3 (0.44 mmol) was required. In the similar experiment 0.375 mmol of NaOH was required to dissolve 0.25 mmol of L-glutamine completely.
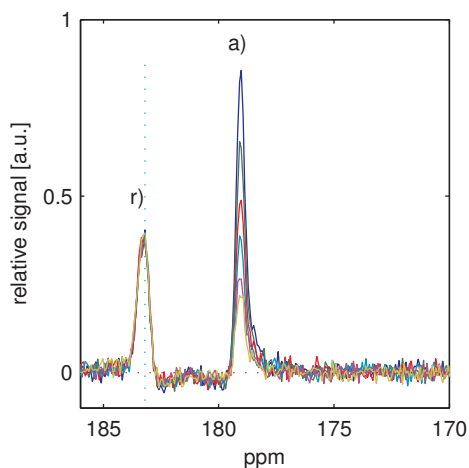
15.1: Spectrum of hyperpolarization decay.   15.2: Thermal polarization spectrum
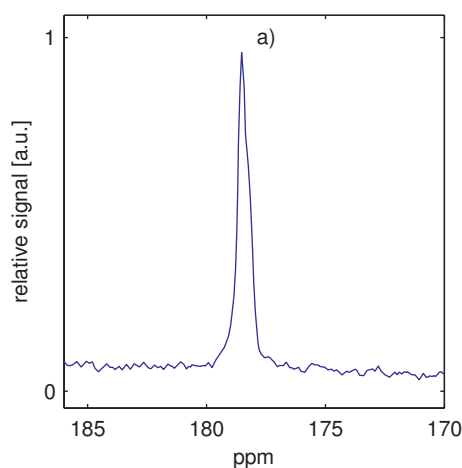
	T_1 at 3T (s)	Solid state signal (a.u.)	Liquid pol. (%)
[5-^{13}C]glutamine	9.3±0.2	16000±1500	0.7±0.02

15.3: Summary of the results acquired from the hyperpolarization spectrum.

Figure 15: Resulting spectra of the experiment with [5-^{13}C]-L-glutamine preparation under basic condition using K_2CO_3 as a base. Notation: a) [5-^{13}C]-L-glutamine, r) ^{13}C-lactate (reference). Each line in the Figure 15.1 represents measurement +5 s after the initiation of the measurement (15 s after dissolution process).

The best performing preparation mixture using K_2CO_3 (8.09M, 55 μL) was analyzed using the 14.1 T NMR spectrometer and the hyperpolarization was measured using the 3 T MRI scanner. The resulted spectra can be seen in the Figure 15.

Due to the fact that maximum solubility of potassium carbonate in water enables maximum concentration of only 8.09 mol/L. The amount required to dissolve 0.50 mmol of glutamine is approximately 0.80 mmol giving ~90 μL, and therefore it is not very suitable preparation technique since, first, the amount of glycerol possible to add is not sufficient to act as a suitable glassing solvent (solid state polarization signal was ~3 times smaller than using NaOH), and second, the lack of glycerol will decrease the viscosity of solvent, and therefore increase the reaction rate to glutamic and pyroglutamic acids.

5.3 INFLUENCE OF THE TEMPERATURE ON GLUTAMINE'S SOLUBILITY

The increased temperature increases the solubility of glutamine, however, it could decrease the viscosity of glycerol, and therefore increase the glutamine solubility even more. The aim was to find out the minimum amount of sodium hydroxide (12M)

required to dissolve 0.25 mmol, respective 0.50 mmol of L-glutamine in 100 μL of glycerol at 70°C.

The aim of this approach was to test the solubility of glutamine in glycerol under basic conditions when the temperature is increased. The test was designed to find the smallest amount of sodium hydroxide able to dissolve 0.25 mmol and 0.5 mmol of glutamine in 100 μL of glassing solvent glycerol. The results are summarized in Table 4 and in Table 5.

NaOH (12M) [μL]	5	10	15	20	25	30	35	40	45	50
L-glutamine [mmol]	0.25	0.25	0.25	0.25	0.25	0.25	0.25	0.25	0.25	0.25
Glycerol [μL]	100	100	100	100	100	100	100	100	100	100
Dissolution time [min]	–	–	–	50	35	20	15	10	10	5

Table 4: Summary of the results of the experiment testing the L-glutamine (0.25 mmol) solubility at the presence of the strong base sodium hydroxide (12M) in 100 μL glycerol at 70°C.

NaOH (12M) [μL]	5	10	15	20	25	30	35	40	45	50
L-glutamine [mmol]	0.50	0.50	0.50	0.50	0.50	0.50	0.50	0.50	0.50	0.50
Glycerol [μL]	100	100	100	100	100	100	100	100	100	100
Dissolution time [min]	–	–	–	–	–	–	55	50	35	20

Table 5: Summary of the results of the experiment testing the L-glutamine (0.50 mmol) solubility at the presence of the strong base sodium hydroxide (12M) in 100 μL glycerol at 70°C.

The results showed that the minimum amount of sodium hydroxide (12M NaOH) required to dissolve 0.25 mmol of L-glutamine in 100 μL of glycerol at 70°C is 20 μL, and 35 μL to dissolve 0.50 mmol of L-glutamine. This means that to dissolve completely 0.25 mmol of L-glutamine 0.3 mmol of NaOH is required in mixture of 100 μL of glycerol and 20 μL of water. To dissolve 0.50 mmol of glutamine within 60 minutes 0.525 mmol of sodium hydroxide is required in mixture of 100 μL of glycerol and 35 μL of H$_2$O. It was clearly demonstrated that the increased temperature decreases the required amount of the base in the solution, and therefore increased the solubility of glutamine compared to the results in Section 5.2.1.

5.4 INFLUENCE OF THE PH AND TEMPERATURE ON GLUTAMINE'S STABILITY

Even though the previous experiments showed that the increased base content and increased temperature enhances the glutamine's solubility, it can also increase the chance that glutamine undergoes a reaction to products of glutamic acid (Glu) and

pyroglutamic acid (pGlu) as described in Section 1.1. The aim of the following experiment was to find out how well the [5-^{13}C]-L-glutamine undergoes the reaction to Glu and pGlu in different conditions.

The best performing preparation techniques from the previous experiments were examined using the NMR measurement of thermal polarization at 14.1 T NMR scanner, and analyzed for the presence of side products of glutamic and pyroglutamic acids (see Fig. 16 for the resulted spectra). From the spectra the amount of resulted side products (Glu, pGlu) were calculated using the comparison of the peak integrals compared to main glutamine peak and the beginning amount of [5-^{13}C]-L-glutamine present.

16.1: [5-^{13}C]glutamine (0.25 mmol, 30°C)   16.2: [5-^{13}C]glutamine (0.50 mmol, 30°C)

16.3: [5-^{13}C]glutamine (0.25 mmol, 70°C)   16.4: [5-^{13}C]glutamine (0.50 mmol, 70°C)
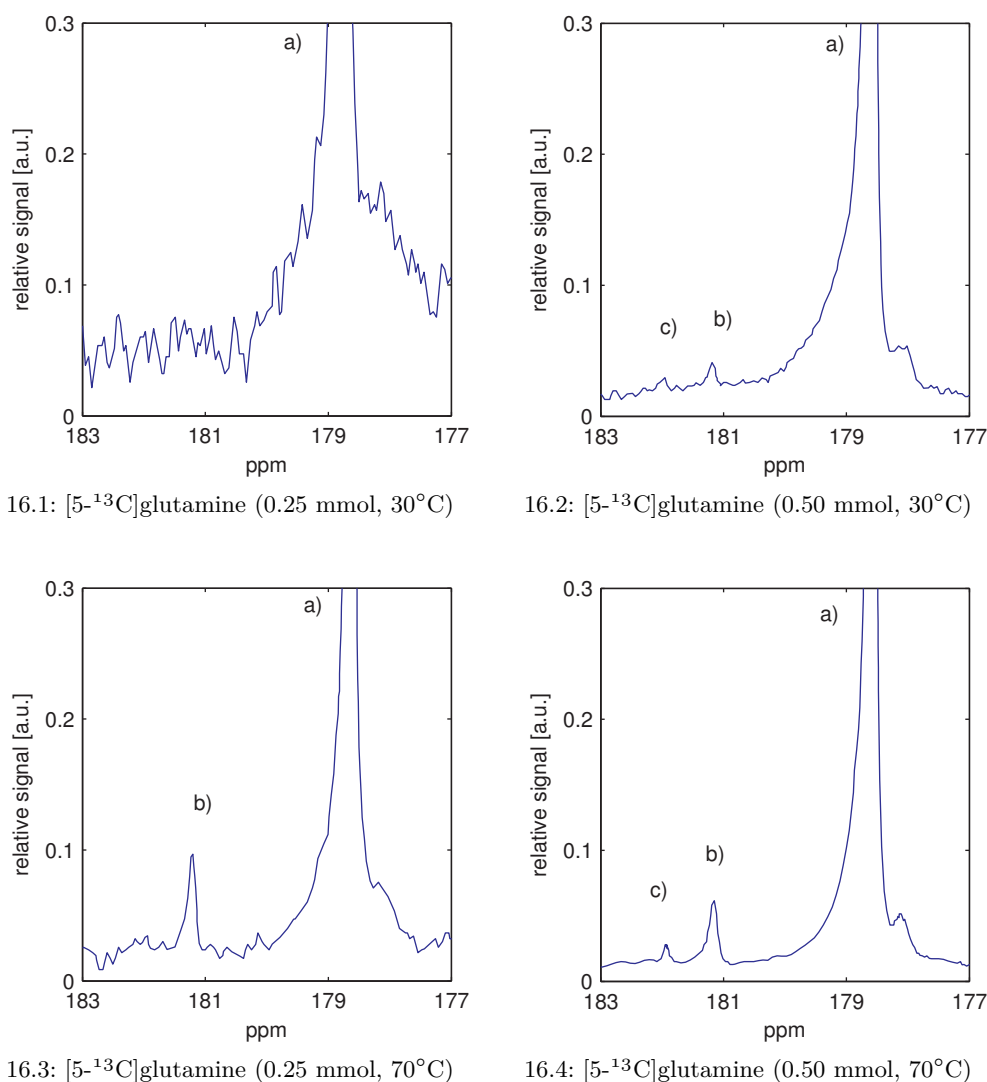
Figure 16: Influence of pH and temperature on the L-glutamine side reactions. The thermal polarization spectra obtained using 14.1 T NMR spectrometer. Notation: a) [5-^{13}C]glutamic acid, b) [5-^{13}C]pyroglutamic acid, c) [5-^{13}C]-L-glutamine.

In the first preparation of [5-¹³C]-L-glutamine (0.25 mmol) at 30°C it was not possible to identify any peak of side products (Fig. 16.1). This means that the final maximum concentration of [5-¹³C]-L-glutamine during the injection would be 50 mmol/L.

In the preparation of [5-¹³C]-L-glutamine (0.50 mmol) at 30°C the side product [5-¹³C]glutamic acid occurred at amount of ~1.4% and [5-¹³C]pyroglutamic acid at the amount of ~2% (Fig. 16.2). This corresponds to 10 μmoles of [5-¹³C]pyroglutamic acid and 7 μmoles of [5-¹³C]glutamic acid, and therefore the maximum final concentration of [5-¹³C]-L-glutamine during injection would be ~96.6 mmol/L.

When the temperature during the preparation process of [5-¹³C]-L-glutamine (0.25 mmol) was increased from 30°C to 70°C, the [5-¹³C]pyroglutamic acid occurred exclusively at the amount of 9.5% resulting in [5-¹³C]-L-glutamine final maximum concentration during injection of ~45.25 mmol/L (Fig. 16.3).

During the preparation of [5-¹³C]-L-glutamine (0.50 mmol) at 70°C the amount of [5-¹³C]-L-glutamine, that underwent the reaction to [5-¹³C]glutamic acid, stayed the same as in preparation at 30°C, however the amount of [5-¹³C]pyroglutamic acid increased, and resulted in the amount of 5%. This means only 70% of [5-¹³C]-L-glutamine would be present in the sample during the possible injection giving the final concentration of ~93.6 mmol/L.

From the results two hypotheses can be deducted. First, if the amount of the sodium hydroxide is increased to allow higher glutamine concentration the amount of glutamic acid increases. This is due to the nucleophilic attack of the hydroxyl group (OH⁻) on the carbonyl group at C-5 position of glutamine and following nucleophilic substitution of the amide group by hydroxyl group forming glutamic acid from glutamine. The proposed reaction mechanism can be seen in Figure 17.
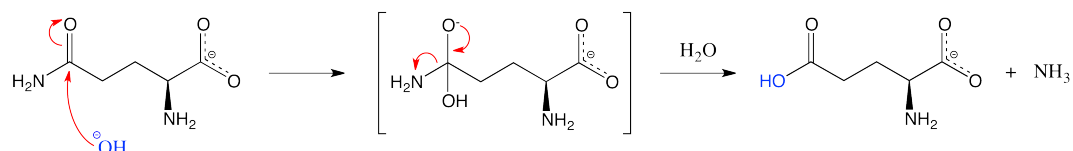
Figure 17: Mechanism of the influence of the pH of the solvent on the stability of L-glutamine. The glutamine under basic conditions undergoes the nucleophilic substitution at carbonyl group at C-5 position resulting in glutamic acid.

Second, if the temperature during the preparation process was increased from 30°C to 70°C, the amount of pyroglutamic acid increased. In this case the mechanism involved the glutamine's amine group, which acted as a nucleophile and attacked the carbonyl group at C-5 position of glutamine making the amide group a good leaving group and form the final product of pyroglutamic acid (see Fig. 18).

Even though the aim of this test was to come up with the preparation technique resulting in no side products, the highest concentration of glutamine was achieved during the preparation of glutamine (0.5 mmol) at 30°C, giving final concentration of ~96.6 mmol/L of [5-¹³C]-L-glutamine, and therefore this preparation technique was hyperpolarized and the hyperpolarization spectra was obtained (see Fig. 20.1).
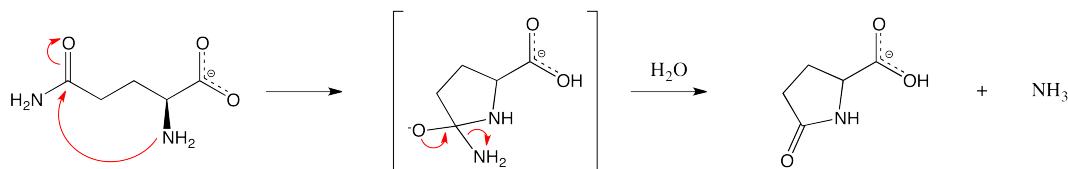
Figure 18: Mechanism of the influence of the solvent's pH on the L-glutamine stability. The glutamine under basic conditions undergoes the nucleophilic substitution at carbonyl group at C-5 position resulting in glutamic acid.

5.5 L-GLUTAMINE SOLUBILITY UNDER ACIDIC CONDITIONS

The third preparation condition, which can increase the solubility of Gln, analyzed was the addition of an acid into the glassing solvent. As a source of hydronium ion (H_3O^+) a strong hydrochloric acid (HCl) was used. Using this approach an aqueous L-glutamine cation is produced. First it was tried to dissolve 0.25 mmol L-glutamine using different amounts of 12M HCl (5 – 50 μL). None of the amounts was able to dissolve the 0.25 mmol of L-glutamine completely, therefore the experiment was inverted and the maximum amount of L-glutamine able to be dissolved by 25 μL of 12M HCl was determined. The summarized results can be seen in Table 6.

L-glutamine [mmol]	0.05	0.07	0.10	0.12	0.14	0.16	0.18	0.20	0.22	0.24
HCl (12M) [μL]	25	25	25	25	25	25	25	25	25	25
Glycerol [μL]	100	100	100	100	100	100	100	100	100	100
Dissolution time [min]	40	45	45	50	50	55	–	–	–	–

Table 6: Summary of the results of the experiment testing the maximum amount of L-glutamine soluble at the presence of different amounts of 12M hydrochloric acid (HCl) added to 100 μL glycerol.

The maximum amount of L-glutamine, which was completely dissolved within 60 minutes was 0.16 mmol. This would give final concentration during injection 32 mmol/L. This does not follow the criteria for successful *in vivo* measurements. Even though this approach is not possible to be used, the sample was analyzed for possible side reaction products using the NMR measurement of thermal polarization at 14.1 T NMR spectrometer. The resulted spectrum can be seen in Figure 19. The spectrum shows that glutamine (peak c) underwent reaction to pyroglutamic acid (peak b) and to unknown compound at 186 ppm (peak a). Due to these results it was decided to discontinue this approach.
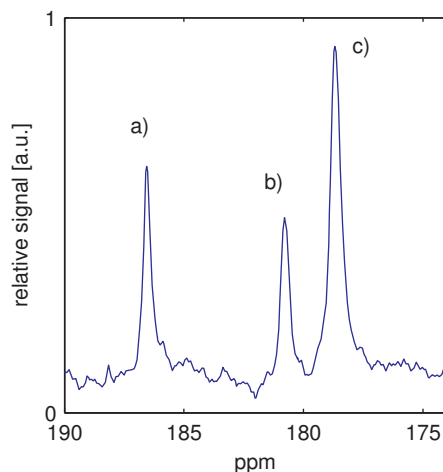
Figure 19: Thermal polarization spectrum of [5-¹³]glutamine sample prepared under acidic conditions. The sample preparation: [5-¹³C]-L-glutamine (0.16 mmol), 12M HCl (25 μL) in glycerol (100 μL). Legend: a) unknown substance, b) pyroglutamic acid, c) glutamine.

5.6 INCREASING THE VISCOSITY OF THE SAMPLE TO SUPPRESS THE SIDE REACTIONS

To decrease the amount of side reactions, which glutamine undergoes under basic condition, the effect of solvent viscosity was examined. The viscosity of the sample was increased by using more concentrated sodium hydroxide, which then decreased the overall amount of water added to the sample and thus increased the viscosity of the sample. This enabled also to increase the final concentration, due to the decrease of the oveall volume of the sample. The maximum solubility of NaOH in water is 1090 g/L at 20°C giving the maximum concentration of 27.25 mol/L. The aim of the experiment was to find out what amount of 27M NaOH is required to dissolve 0.50 mmol of L-glutamine in 100 μL of glycerol. The gained results are summarized in Table 7.

NaOH (27M) [μL]	5	10	15	20	25	30	35	40	45	50
L-glutamine [mmol]	0.50	0.50	0.50	0.50	0.50	0.50	0.50	0.50	0.50	0.50
Glycerol [μL]	100	100	100	100	100	100	100	100	100	100
Dissolution time [min]	–	–	–	–	–	50	50	45	45	40

Table 7: Testing of the solubility of glutamine increased by strong base to find a minimum concentration of 27 M NaOH required to dissolve glutamine giving 100 mM solution (0.50 mmol).

The results showed that 30 μL of 27M NaOH (0.81 mmol) were suitable to dissolve 0.50 mmol of L-glutamine completely within 60 minutes. The amount of sodium hy-
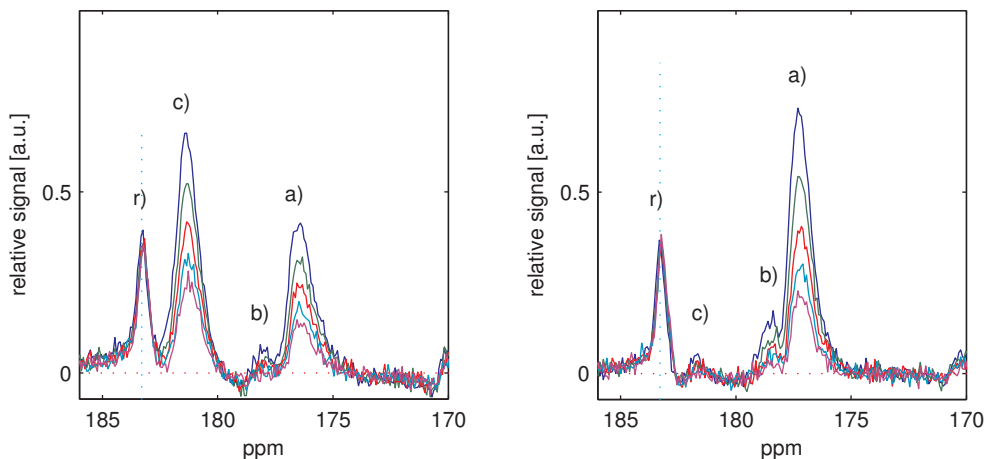
20.1: Spectrum of the sample dissolved by 12M NaOH

20.2: Spectrum of the sample dissolved by 27M NaOH.

	T_1 at 3T (s)	Solid state signal (a.u.)	Liquid pol. (%)
1) [5-¹³C]-L-glutamine	9.2±0.3	15000±400	0.07±3×10⁻³
2) [5-¹³C]-L-glutamine	8.9±0.2	15500±300	0.06±6×10⁻³

20.3: Summary of the results acquired from the hyperpolarization spectrum.

Figure 20: Comparison of hyperpolarized spectra of 12M NaOH and 27M NaOH approaches obtained using the 3 T MRI scanner. Notation: a) [5-¹³C]-L-glutamine, b) [5-¹³C]pyroglutamic acid, c) [5-¹³C]glutamic acid, r) ¹³C-lactate (reference). Each line represents measurement +5 s after the initiation of the measurement (17 s after dissolution process).

droxide required increased compared to 12M NaOH experiments, where 0.675 mmol was required. The overall volume of the sample decreased, because in this case the water added to 100 μL of glycerol was 30 μL compared to 45 μL in case of 12M NaOH.

The sample was hyperpolarized and the spectrum was measured at 3 T MRI scanner (see Fig. 20.2). In the Figure 20 the approach with 12M NaOH and 27M NaOH are compared. The usage of 27M NaOH dramatically decreased the presence of glutamic acid (Glu) in the sample (peak c), however, very slightly increased the amount of pyroglutamic acid. When summarized the usage of 27M NaOH has been found as a better approach due to the increase of glutamine in the sample.

5.7 LOSS OF THE HYPERPOLARIZATION IN THE LIQUID STATE

5.7.1 *Comparison of [5-¹³C]glutamine and L-glutamine hyperpolarization*

Due to the fact that the liquid-state polarization obtained was in ppt and not in percentages a test comparing the hyperpolarization of [5-¹³C]-L-glutamine and
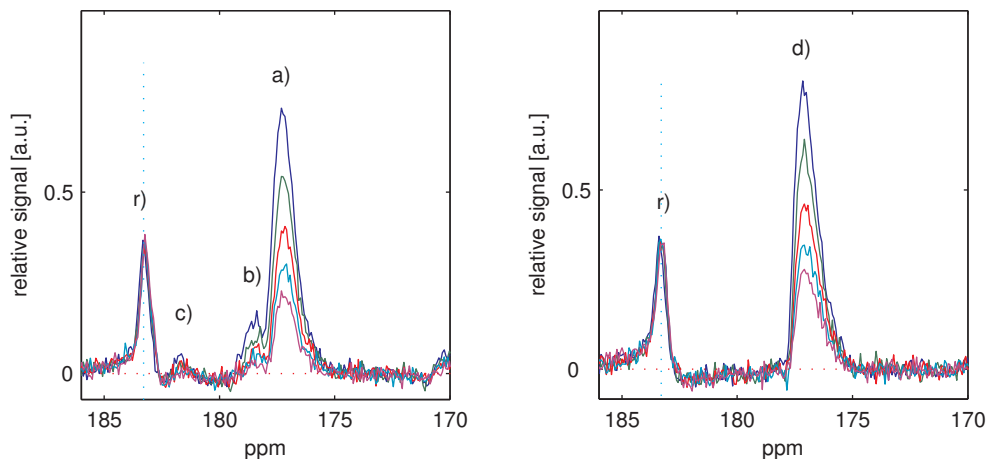
21.1: Spectrum of hyperpolarization decay of [5-¹³C]-L-glutamine sample.

21.2: Spectrum of hyperpolarization decay of L-glutamine sample.

	T_1 at 3T (s)	Solid state signal (a.u.)	Liquid pol. (%)
(1) [5-¹³C]-L-glutamine	8.9±0.2	15500±300	0.06±6×10⁻³
(2) L-glutamine	8.7±0.4	2100±200	0.06±4×10⁻³

21.3: Summary of the results acquired from the hyperpolarization spectra.

Figure 21: Comparison of hyperpolarized spectra of [5-¹³C]-L-glutamine and naturally abundant L-glutamine using the 3 T MRI scanner. Notation: a) [5-¹³C]-L-glutamine, b) [5-¹³C]pyroglutamic acid, c) [5-¹³C]glutamic acid, d) L-glutamine, r) ¹³C-lactate (reference).Each line represents measurement +5 s after the initiation of the measurement (17 s after dissolution process).

L-glutamine was performed. The resulted spectra can be seen in Figure 21. The hyperpolarization obtained for both compounds was very similar giving the liquid-state polarization of [5-¹³C]-L-glutamine 0.06±6×10⁻³% and of L-glutamine 0.06±4×10⁻³% even though their solid state polarization is very different giving almost 7× higher value for the [5-¹³C]-L-glutamine. Both refer to the hyperpolarization of ¹³C atoms present in both molecules even though there is only naturally abundant 1.1% of ¹³C-L-glutamine present in the L-glutamine sample, and there are 5 possible position for the ¹³C atom to be present. This proofed our prediction, that there must be some force, which enables a very fast relaxation of the [5-¹³C]-L-glutamine signal when present in liquid–state.

5.7.2 *Metal analysis*

The presence of impurities such as ferromagnetic metals (e. g.Cu, Ni) could be the reason of fast relaxation of [5-¹³C]-L-glutamine in liquid state. These metals could have been used during the synthesis of [5-¹³C]-L-glutamine and their residue might have
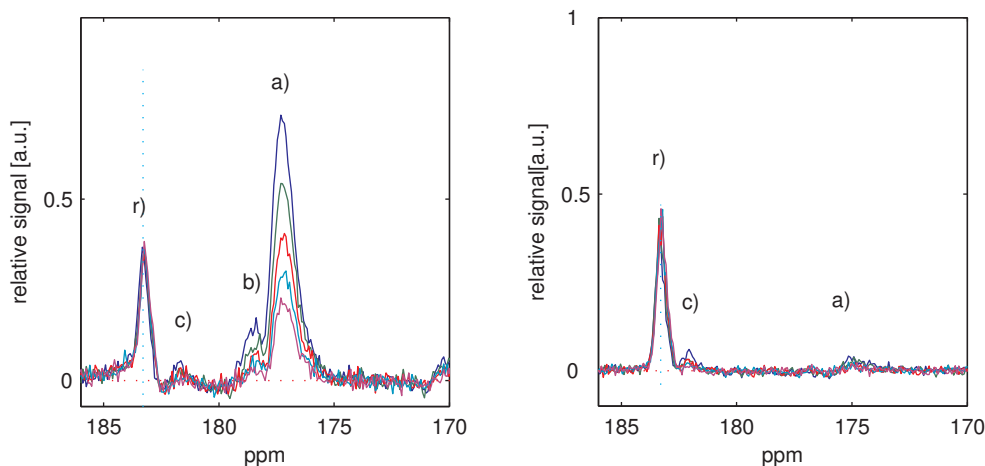
22.1: Spectrum of hyperpolarization decay of [5-¹³C]-L-glutamine (Sigma-Aldrich, St. Louis, MO, USA)

22.2: Spectrum of hyperpolarization decay [5-¹³C]-L-glutamine (Cambridge Isotope Laboratories, Andover, MA, USA)

	T_1 at 3T (s)	Solid state signal (a.u.)	Liquid pol. (%)
1) [5-¹³C]-L-glutamine (Sigma-Aldrich)	8.9±0.2	15500±300	0.06±6×10⁻³
2) [5-¹³C]-L-glutamine (Cambridge Isot.)	–	–	–

22.3: Summary of the results acquired from the hyperpolarization spectra.

Figure 22: Comparison of hyperpolarization spectra of [5-¹³C]-L-glutamine (Sigma-Aldrich, St. Louis, MO, USA), and [5-¹³C]-L-glutamine (Cambridge Isotope Laboratories, Andover, MA, USA) Notation: a) [5-¹³C]-L-glutamine, b) [5-¹³C]pyroglutamic acid, c) [5-¹³C]glutamic acid, d) L-glutamine, r) ¹³C-lactate (reference). Each line represents measurement +5 s after the initiation of the measurement (17 s after dissolution process).

been still present in the sample even in very small amounts. The [5-¹³C]-L-glutamine was ordered from all available suppliers, which had [5-¹³C]-L-glutamine on market: a) Sigma-Aldrich Co. LLC (St. Louis, MO, USA); b) Cambridge Isotope Laboratories, Inc (Andover, MA, USA); c) Toronto Research Chemicals (Ontario, Canada). However, only Sigma-Aldrich Co. and Cambridge Isotope Laboratories were able to deliver their product. The obtained samples were analyzed in the Chemical and Structural Analysis Laboratory (GE Global Research, General Electric Company, Niskayuna, NY, USA) using the High Resolution Inductively Coupled Plasma Mass Spectrometry (HR-ICP-MS).

The results are summarized in the Table 8. For our purposes the results of the amounts of the ferromagnetic metals such as titanium (Ti), manganese (Mn), iron (Fe), cobalt (Co), nickel (Ni), copper (Cu), zinc (Zn), molybdenum (Mo), and gadolinium (Gd).

From the chemical elements of interest the amount of the Mn, Fe, Co, and Gd were below the detection limit in both of the samples. The amount of Mo were detected in

	[5-^{13}C]-L-glutamine			[5-^{13}C]-L-glutamine	
	Cambridge Is.	Sigma-Aldrich		Cambridge Is.	Sigma-Aldrich
^{7}Li	<0.90	1.19±0.03	^{111}Cd	<0.2	<0.15
^{9}Be	<0.90	<0.90	^{115}In	<0.025	<0.025
^{11}B	1.56±0.02	3.92±0.08	^{125}Te	<0.3	<0.3
^{23}Na	10±1	152±1	^{137}Ba	0.26±0.06	0.25±0.05
^{25}Mg	2.5±0.4	3.3±0.7	^{139}La	<0.09	<0.09
^{27}Al	1.8±0.4	2.0±0.3	^{140}Ce	<0.03	<0.03
^{44}Ca	9±1	8±2	^{141}Pr	<0.015	<0.015
^{45}Sc	<0.12	<0.12	^{146}Nd	<0.015	<0.015
^{47}Ti	0.09±0.02	0.15±0.04	^{147}Sm	<0.09	<0.09
^{51}V	0.056±0.007	0.067±0.008	^{151}Eu	<0.03	<0.03
^{52}Cr	<0.6	<0.8	^{155}Gd	<0.03	<0.03
^{55}Mn	<0.3	<0.3	^{159}Tb	<0.15	<0.15
^{57}Fe	<6	<6	^{163}Dy	<0.015	<0.015
^{59}Co	<0.06	<0.06	^{165}Ho	<0.03	<0.03
^{62}Ni	0.17±0.05	1.82±0.04	^{166}Er	<0.003	<0.003
^{63}Cu	0.12±0.02	0.85±0.04	^{169}Tm	<0.03	<0.03
^{66}Zn	0.6±0.1	0.7±0.2	^{172}Yb	<0.15	<0.15
^{69}Ga	<0.2	<0.2	^{175}Lu	<0.006	<0.006
^{75}As	<1.5	<1.5	^{177}Hf	<0.3	<0.3
^{77}Se	19±2	19±2	^{182}W	<0.3	<0.3
^{85}Rb	<0.06	<0.06	^{185}Re	<0.02	<0.02
^{88}Sr	0.17±0.04	<0.15	^{205}Tl	<0.03	<0.03
^{89}Y	<0.009	<0.009	^{208}Pb	<0.03	<0.03
^{90}Zr	<0.25	<0.25	^{209}Bi	<0.06	<0.06
^{93}Nb	<0.2	<0.2	^{232}Th	<0.09	<0.09
^{97}Mo	0.26±0.04	0.18±0.07	^{238}U	<0.03	<0.03
^{109}Ag	0.22±0.04	<0.2			

Table 8: Metal Analysis of [5-^{13}C]-L-glutamine from different suppliers by solution HR-ICP-MS. Results are expressed as μg/mL (ppm) of analyte in the sample as received ± the 95% confidence intervals (CI).

both sample with very similar results of 0.26±0.04 μg/mL for the [5-^{13}C]-L-glutamine (Sigma-Aldrich Co., St. Louis, MO, USA) and 0.18±0.07 μg/mL for the [5-^{13}C]-L-glutamine (Cambridge Isotope Laboratories, Andover, MA, USA). There was also no significant difference between the samples in case of the Ti and Zn amount even though there was measured slightly higher amount in the [5-^{13}C]-L-glutamine (Sigma-Aldrich, St. Louis, MO, USA).

Even though there was no significant difference in the majority of the elements analyzed, there were two elements with significant differences in concentrations: Ni and Cu. In the [5-^{13}C]-L-glutamine (Sigma-Aldrich, St. Louis, MO, USA) there was 10 times more Ni (1.82±0.04 μg/mL vs. 0.17±0.05 μg/mL), and 7 times more Cu (0.85±0.04 μg/mL vs. 0.12±0.02 μg/mL) than in the [5-^{13}C]-L-glutamine (Cambridge Isotope Laboratories, Andover, MA, USA).

Due to this analysis the concentration of Cu and Ni in the [5-^{13}C]-L-glutamine supplied by Sigma-Aldrich (St. Louis, MO, USA) was identified as a possible reason for the fast relaxation of the hyperpolarization in the liquid state, and therefore for the loss of the signal during the measurement. The [5-^{13}C]-L-glutamine (Cambridge Isotope Laboratories, Andover, MA, USA) was hyperpolarized and its hyperpolarization was measured at 3 T MRI scanner. As shown in Figure 22.2 no signal was obtained. This measurement was repeated several times with the same results even though that the solid state polarization was the same as in the case of [5-^{13}C]-L-glutamine supplied by Sigma-Aldrich (St. Louis, MO, USA). These results gave us a clue that the impurities are not the only reason for fast relaxation of [5-^{13}C]-L-glutamine hyperpolarization in solution.

5.7.3 *Loss of the signal due to the molecule's nature*

To prove that the loss of the signal is not due to any additional impurities and elements present in the sample, but caused intrinsic properties of the molecule a test was designed where [5-^{13}C]-L-glutamine was forced to undergo the reaction to [5-^{13}C]glutamic acid completely. This was done using a high concentration NaOH via the S$_N$2t mechanism described in Figure 17. The obtained hyperpolarization spectrum was compared to the hyperpolarization spectrum of synthesized [5-^{13}C]glutamic acid (Cambridge Isotope Laboratories, Andover, MA, USA).

The resulting spectra in Figure 23 show that the obtained hyperpolarization for both tested samples were very similar, and therefore one could summarize that the loss of the hyperpolarization of [5-^{13}C]-L-glutamine is not due to the impurities in the sample, or any other components introduced during the preparation, but is due to the nature of the glutamine molecule.

5.7.4 *Loss of polarization due to relaxation through scalar coupling (type II scalar relaxation)*

Due to the presence of ^{14}N in the amide group bonded to ^{13}C-5, one of the possible explanation of the signal loss in liquid state was a relaxation through scalar coupling (type II). The contributions of other relaxation mechanisms such as dipole–dipole interaction (R_1^d), spin-rotation (R_1^{sr}), and chemical shift anisotropy (R_1^{csa}) were determined to be negligible after consideration of the temperature (298 – 310 K) and magnetic-field (3.0 – 14.1 T) dependencies of T_1. The paramagnetic contribution (R_1^{para}) can also potentially affect a hyperpolarized substrate, however, Mielville et
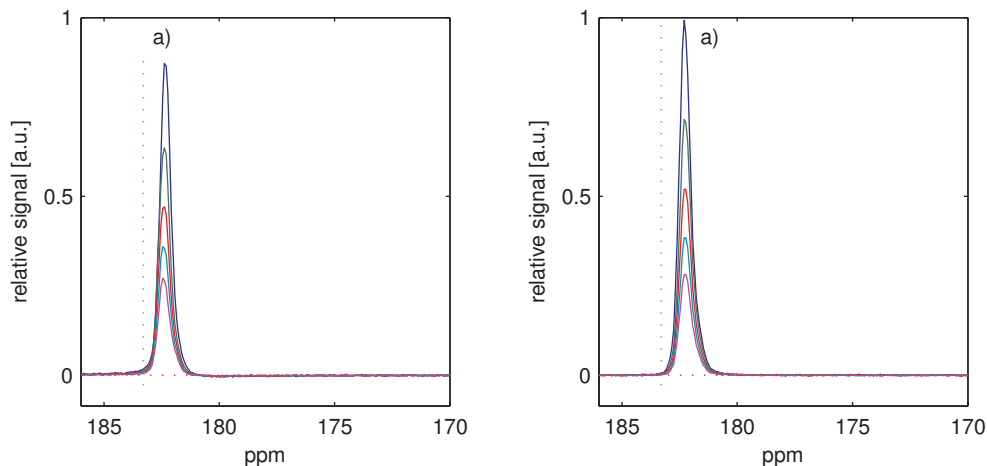
23.1: Spectrum of hyperpolarization decay of [5-¹³C]glutamic acid from Gln

23.2: Spectrum of hyperpolarization decay of synthetized [5-¹³C]glutamic acid

	T_1 at 3T (s)	Solid state signal (a.u.)	Liquid pol. (%)
1) [5-¹³C]glutamate (from Gln)	16.5±0.2	1300±100	64.1±0.3
2) [5-¹³C]glutamate (synthesized)	16.1±0.2	1400±200	62.2±0.2

23.3: Summary of the results acquired from the hyperpolarization spectra.

Figure 23: Comparison of the hyperpolarized spectra of synthetized [5-¹³C]glutamic acid (Cambridge Isotope Laboratories, Andover, MA, USA) and [5-¹³C]-L-glutamine (Cambridge Isotope Laboratories, Andover, MA, USA) under highly basic conditions which fully underwent reaction to [5-¹³C]glutamic acid. Notation: a) [5-¹³C]glutamic acid. Each line represents measurement +5 s after the initiation of the measurement (15 s after dissolution process).

al. (2011) reported that this effect is negligible when using a trityl radical (such as OX063) because the contact distance between the radical center and the substrate is larger than in nitroxide radicals like TEMPO [118].

In order to assess the influence of external field dependent relaxation mechanisms, first the magnetic field present along the pathway of the sample during the transport from DNP polarizer to MRI scanner was determined. In Figure 24, the measured magnetic field is plotted along the travel path. At ~2.2 m a large increase of the magnetic field was observed (peak b). This was due to the position of the collection flask during the dissolution process, which was placed near by the built-in magnet at the top of the DNP polarizer.

The $J_{^{13}C-^{14}N}$ values for [5-¹³C]-L-glutamine were calculated to be 11.3±0.1 Hz, and the T_1 of ¹⁴N was 1.0±0.1 ms [119]. The R_1^{sc} contribution was calculated using Equation 6 and plotted along the transport path (see Fig. 25) The sample traveled at a constant speed from the polarizer to the collection flask (~1 m/s), remained static for ~3 s in the collection flask, and then was transported by human force from

the collection flask to the MRI scanner in NMR tube at a speed of (~1.5 m/s). To calculate the mean relaxation rate during transport (Eq. 6), a weighted average of the values in Fig. 25 was calculated taking into account the time that the sample remained at each position; this calculation resulted in a mean relaxation rate value of 0.98±0.05 s^{-1}. An analogous calculation gave a weighted mean magnetic field of 0.7 mT.

To proof that the contribution of relaxation through scalar coupling is responsible for the fast signal decay four different experiments were performed. First, [5-^{13}C]-L-glutamine was transported with and without a 0.2 T permanent magnet attached to the NMR tube during the transport from the polarizer to the MRI scan-
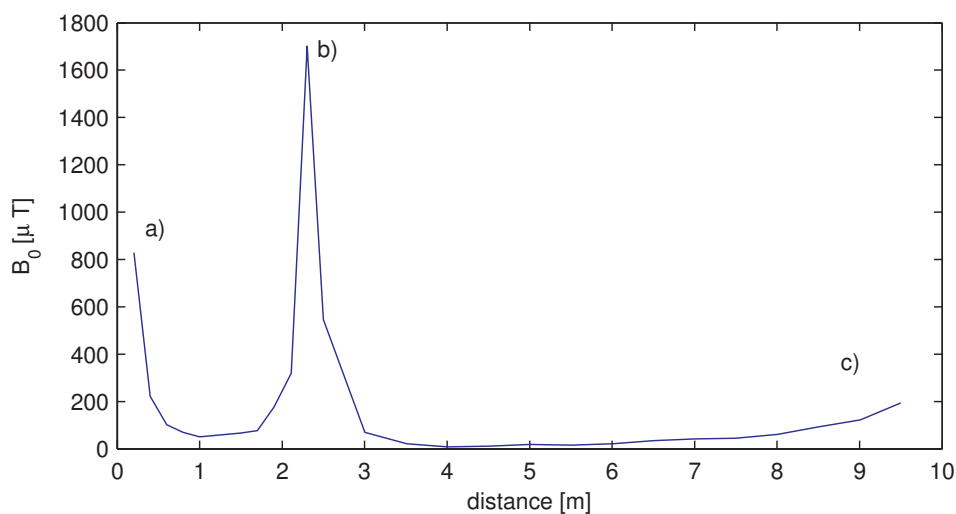
Figure 24: Magnetic field strength along the path from the polarizer bore to the open MRI scanner room door. Notation: a) Leaving the DNP magnet bore, b) Collection flask, c) Entering the MRI scanner room.
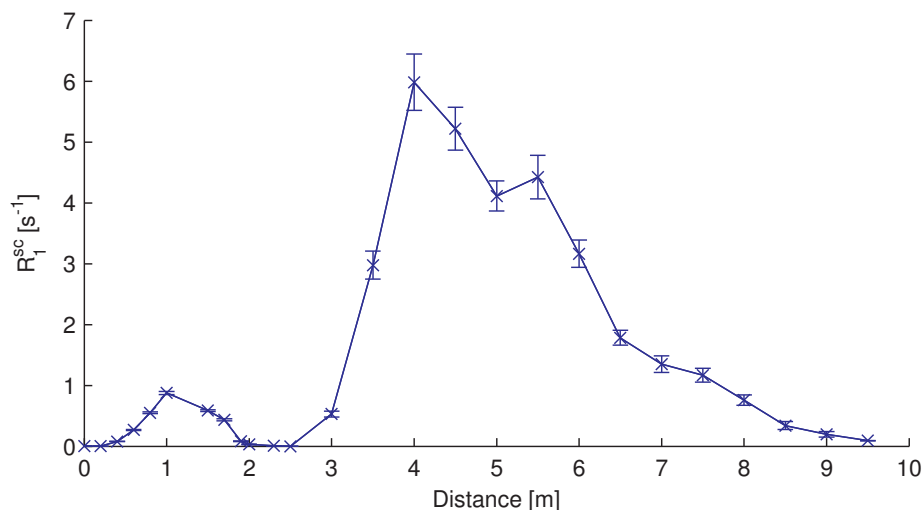
Figure 25: ^{13}C relaxation rate arising from the scalar coupling contribution estimated from the measured B^{o}, J$_{C-N}$, and ^{14}N T_1 values.

26.1: [5-^{13}C]-L-glutamine transported in Earth's magnetic field.

26.2: [5-^{13}C]-L-glutamine attached to 0.2 T permanent magnet during transport.

26.3: [5-^{13}C,^{15}N]-L-glutamine transported in Earth's magnetic field.

26.4: [5-^{13}C,^{15}N]-L-glutamine attached to 0.2 T permanent magnet during transport.
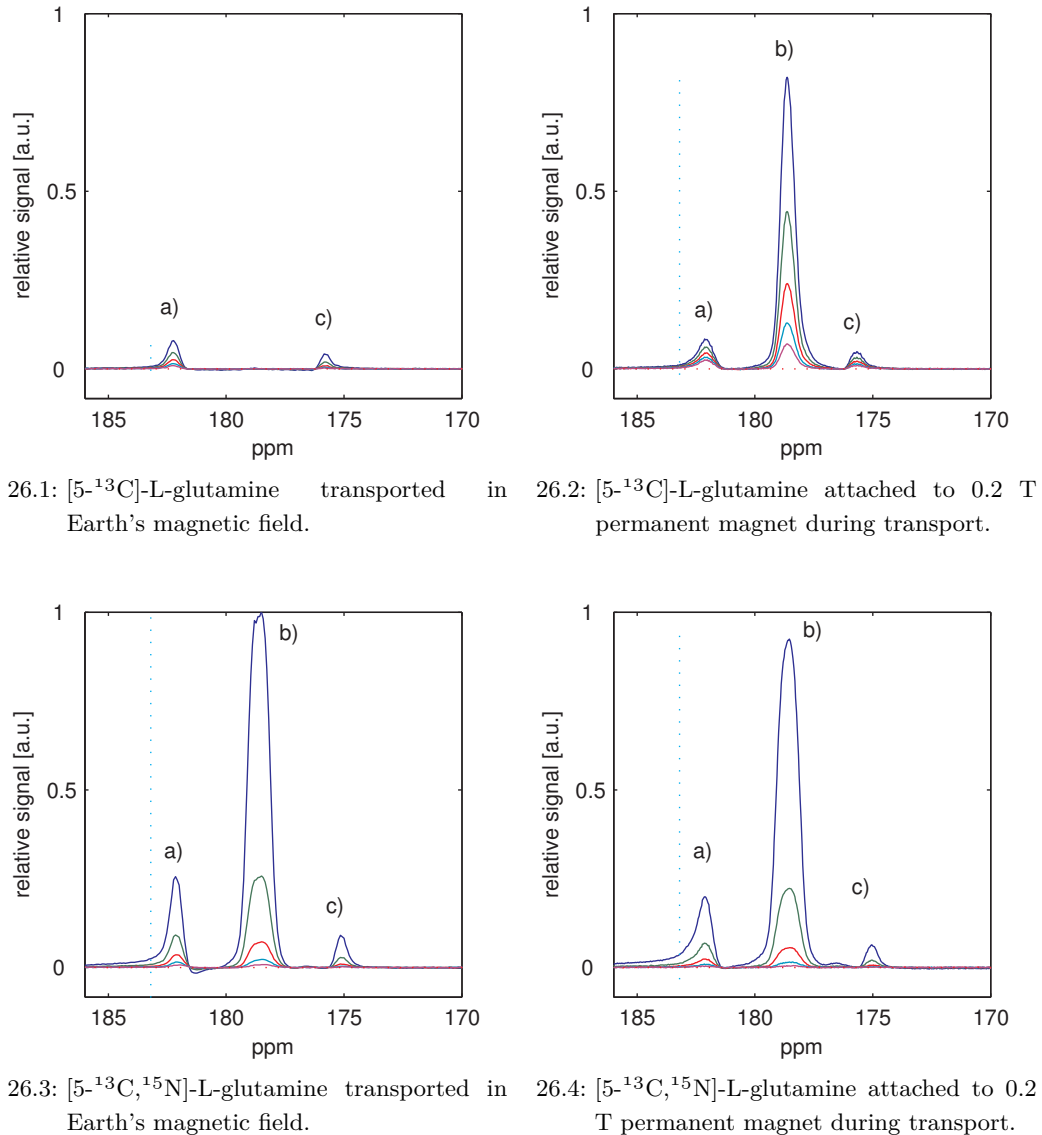
Figure 26: Results of the experiment testing for relaxation through scalar coupling (type II). Notation: a) [5-^{13}C]glutamic acid, b) [5-^{13}C]-L-glutamine, c) [5-^{13}C]pyroglutamic acid. Each line represents measurement +5 s after the initiation of the measurement (17 s after dissolution process).

ner. To assess the role of the coupling of ^{13}C on C-5 position to the amide ^{14}N, [5-^{13}C,^{15}N]-L-glutamine with ^{15}N in the amide group was examined in the same way as [5-^{13}C]-L-glutamine – with and without 0.2 T permanent magnet attached during the transport from DNP polarizer to MRI scanner. The resulting spectra are shown in Figure 26. In Table 9, the resulting polarization values are summarized.

Significant increase in the liquid state polarization was observed, when sustainable sufficiently high magnetic field was applied during the transport from the DNP polarizer to the MRI scanner. As expected, no significant polarization changes were observed when the same experiments were performed on glutamine with a ^{15}N labeled

	T_1 (s)	Earth's magnetic field		0.2 T permanent magnet	
	at 3.0 T	Solid state signal (a.u.)	Liquid pol. (%)	Solid state signal (a.u.)	Liquid pol. (%)
[5-^{13}C]glutamine	8.0±0.1	3500±200	0.02±5×10^{-3}	3700±450	0.7±0.1
[5-^{13}C,^{15}N]Gln	7.7±0.4	3600±300	0.7±0.2	3600±300	0.8±0.2

Table 9: Results of the experiment testing for relaxation through scalar coupling (type II).

amide group. In fact, given the dependence of $T_1(sc)$ on the T_1 of the coupled nucleus (Eq. 6) only quadrupolar ^{14}N-containing molecules with a short T_1 are affected by this mechanism.

This confirms the hypotheses that the relaxation through scalar coupling at low magnetic field is the main contributor to the observed relaxation rate. The polarization values have not been corrected for polarization losses due to polarization decay during the transfer since this is outside of the scope of the study. Furthermore, in our case, the T_1 cannot be considered constant during transport, which complicates any potential corrections and makes them unreliable.

Part IV

DISCUSSION

*The best idea is the one
that always leaves a loophole for the possibility
that everything is at the same time
completely different.*

— Václav Havel

DISCUSSION

6.1 ANALYSIS OF THERMAL POLARIZATION SPECTRA

From the thermal polarization spectra obtained using the 14.1 T NMR described in Figure 16 on page 45 side products of [5-^{13}C]pyroglutamic acid (pGlu) and [5-^{13}C]glutamic acid (Glu) were assigned to the chemical shifts 181.3 ppm and 182.0 ppm, respectively. Since the sample included sodium hydroxide (NaOH) was dissolved in 2 mL of D$_2$O, the pH was alkaline and therefore could have affected the obtained chemical shifts. The chemical shift of [5-^{13}C]glutamic acid is dependent on pH due to the presence of charged hydroxyl group (OH$^-$) near the C-5 labeled glutamine's ^{13}C-carbon. The chemical shift moves from 177.83 (D$_2$O) at pH=3.34 through 182.05 (D$_2$O, pH=7.01) to 182.91 (D$_2$O, pH=9.86) [120]. However, there are no references for the chemical shift pH dependency of [5-^{13}C]pyroglutamic acid. According to Spectral Database for Organic Compounds the chemical shift in D$_2$O is 182.6 ppm, however, there is no peak in this region obtained [120]. Even though the pGlu content is highly probable, it cannot be with high certainty said which of the peaks belong to it.

In Section 5.4 on page 44 we summarized that temperature influence on the glutamine was that the if temperature was increased, and therefore the viscosity of glycerol decreased, it also enhanced the reaction rate of Gln to pGlu. However, if the peak, which was first referred to pGlu belongs actually to Glu, the explanation would still be true, because the Glu also undergoes a reaction to pGlu via mechanism showed in Figure 27. To summarize, there is an uncertainty in the assignment of the chemical shifts, which does not affect the general conclusion with respect to the reaction rates.
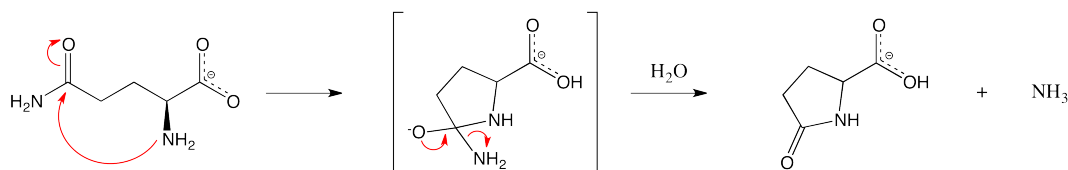
Figure 27: Mechanism of the influence of the solvent's pH on the L-glutamine stability. The glutamine under basic conditions undergoes the nucleophilic substitution at carbonyl group at C-5 position resulting in glutamic acid.

6.2   EFFECT OF THE [5-¹³C]-L-GLUTAMINE LOSS OF THE SIGNAL ON THE ANALYSIS OF DATA

The experiments in Section 5.7.4 (Loss of polarization due to relaxation through scalar coupling (type II scalar relaxation)) showed that the hyperpolarization of [5-¹³C]-L-glutamine was lost during the transport through Earth's low magnetic field between the DNP polarizer and the MRI scanner in all previous experiments. If we include this knowledge into the analysis of previously obtained spectra, which were used for the enhancing the sample preparation technique before polarization, new conclusions can be drawn.

The experiments, where the [5-¹³C]-L-glutamine was transported at sustainably high magnetic field, showed that the peak of [5-¹³C]pyroglutamic acid is at 175.5 ppm. This is a very different chemical shift from obtained thermal polarization spectrum in Figure 16 on page 45. There could be different influence of chemical shift such as presence of glycerol, trityl radical, TRIS buffer, or other. However the peak at chemical shift of ~175 ppm was observed in majority of the obtained spectra, and it was assigned to [5-¹³C]pyroglutamic acid due to the fact that [5-¹³C]glutamic acid was present at ~182.0 (see Fig. 23 on page 54) and therefore the second observed peak was with high probability the [5-¹³C]pyroglutamic acid. If we consider this as a fact, all the hyperpolarization spectra obtained during the sample preparation must be analyzed again.

6.2.1   *Usage of 27M NaOH instead of 12M NaOH*

In Figure 20 on page 49 hyperpolarization spectrum of preparation involving 12M NaOH is compared to hyperpolarization spectrum of preparation involving 27M NaOH. In both of the spectra there are two peaks at chemical shifts of ~176 ppm and ~181 ppm. Due to the findings described in Section 6.2 we can with high probability assign the peak at chemical shift of ~176 ppm to [5-¹³C]pyroglutamic acid and at ~181 ppm to [5-¹³C]glutamic acid.

Therefore with the new analysis approach of the spectra (see Fig. 20 on page 49) we can conclude that the sample preparation involving 27M NaOH has an important influence on the reaction rate of [5-¹³C]-L-glutamine to [5-¹³C]glutamic acid. The reaction rate is decreased to minimum. On the other hand the signal of [5-¹³C]pyroglutamic acid slightly increased.

With the new conclusion we can say that the usage of 27M NaOH is better than 12M NaOH because glutamic acid is the less desired side product compared to pyroglutamic acid due to the fact that [5-¹³C]glutamic acid is the first intermediate of [5-¹³C]-L-glutamine metabolism *in vivo*, and therefore injecting [5-¹³C]glutamic acid with [5-¹³C]-L-glutamine would be very contra-productive.

6.2.2 *Comparison of [5-¹³C]-L-glutamine with L-glutamine*

In the next experiment, where the [5-¹³C]-L-glutamine hyperpolarization signal was compared to naturally abundant L-glutamine described in Figure 21, there is actually no [5-¹³C]-L-glutamine peak present due to the loss of the signal by relaxation through scalar coupling (type II), but actually the hyperpolarization signal of [5-¹³C]pyroglutamic acids were compared.

However, even though if it is pyroglutamic acid, there should be much higher hyperpolarization signal in case of the ¹³C-labelled compound due to the fact that in the naturally occurring there is only 1.1% of the ¹³C-carbon, and not to mention this carbon can be present it any of all C-5 positions. The low signal of [5-¹³C]pyroglutamic acid hyperpolarization signal can be explained by the presence of the copper and nickel in the sample described in Section 5.7.2, or by better stability of the labeled compound.

6.3 ISOMERISM

All the amino acids involved in human metabolism are the specifically L-isomers including the L-glutamine. Due to the fact that glutamine is treated with an excess of base (sodium hydroxide), and several side reactions to glutamic acid and pyroglutamic acid might occur, the L-isomers can undergo a reaction forming their D-isomer (i. e. racemization). However, unlike other D-isomers of amino acids neither D-glutamine nor D-glutamic acid are poisonous to humans and they are actually metabolized by the same enzymes as their L-isomers or could be converted back to them. As described in Figure 28 L-glutamine when metabolised can be actually enzymatically converted to is D-form using amino acid racemase (5.1.1.10). This chemical reaction is reversible and therefore the D-glutamine can be also converted into its L-isomer. The same is true for glutamic acid. Both isomers can be converted into each other by Glutamate racemase (5.1.1.3). L-glutamine and D-glutamine are both transformed into glutamic acid isomers by the same enzymes: Glutaminase (3.5.1.2) and glutamin(aspagin-)ase (3.5.1.38). In summary we can say that D-isomer of glutamine or glutamic acid are not an issue during the measurement if they occur in small amounts.

6.4 LOW LIQUID-STATE POLARIZATION DURING EXPERIMENTS INVESTIGATING SCALAR COUPLING INFLUENCE

Even though we proved that the relaxation through scalar coupling is responsible for the fast decay of the liquid-state polarization and provided two possible ways of solving this issue, the resulted polarization and T_1 were still smaller than in literature. The measured values were 0.7±0.1% for the polarization and the T_1 was calculated to be 8.0±0.1 s for [5-¹³C]-L-glutamine (see Table 9 for references). The values obtained
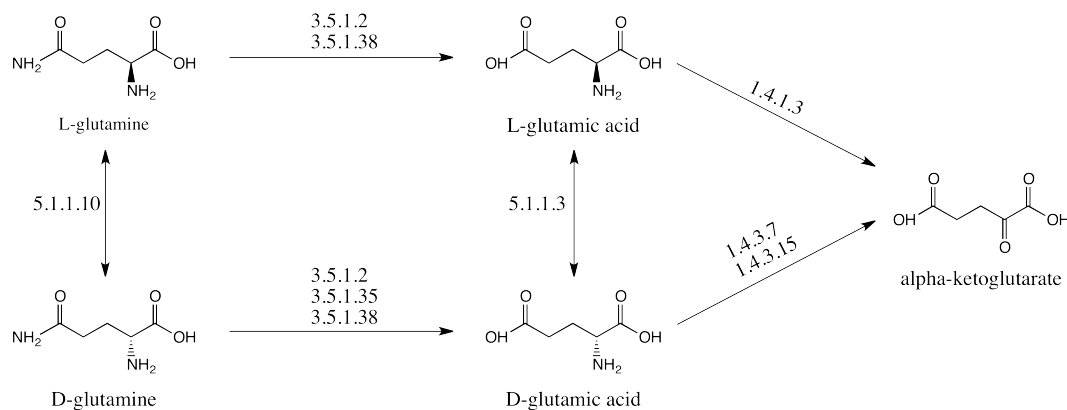
Figure 28: Metabolism of L-glutamine and D-glutamine. List of involved enzymes: 1.4.1.3: glutamate dehydrogenase, 1.4.3.7: D-glutamate oxidase, 1.4.3.15: D-glutamate(D-aspartate) oxidase, 3.5.1.2: glutaminase, 3.5.1.35: D-glutaminase, 3.5.1.38: glutamin-(asparagin-)ase, 5.1.1.3: Glutamate racemase, 5.1.1.10: amino-acid racemase. (Based on information from [121])

previously by Gallagher et al. (2008) showed that glutamine with labeled ^{13}C on C-5 position could be polarized up to 5% and the obtained T_1 was 16.1 s [116].

There are several factors that might have had an influence on the resulted data, i. e. homogenity of the sample mixture, however, from the results especially from the low solid-state polarization compared to the previous approaches, the most possible explanation is a low amount of the glutamine compared to the constant amount of the trytil radical and contrasting agent. As of to date there are no studies that might support these hypotheses and therefore this phenomenon might be interesting to investigate in future attempts.

6.5 FUTURE AIMS

In the future there are several possible aims, which should be experimentally studied. Since the preparation technique has been optimized, the *in vitro* and *in vivo* experiments are naturally the next possible step in the investigation. The molecule can also be modified for better stability by attaching a acetyl group on the amine nitrogen, or using deuterated [5-^{13}C-4-^{2}H$_2$]glutamine for better polarization results.

6.5.1 *In vitro and in vivo experiments*

Due to the fact that the preparation technique for [5-^{13}C]-L-glutamine has been optimized and fully developed, one of the first goals will be to continue with the aims of this thesis and proceed with *in vitro* experiments. This will be performed on cancer cell cultures (such as cultures of HCC cells).

Whereas *in vitro* experiments has been already performed with [5-^{13}C]-L-glutamine, only recently Cabella et. al. published the first *in vivo* application of [5-^{13}C]-L-glutamine with very promising results [122]. The next approach will be

to investigate the metabolism of [5-¹³C]-L-glutamine on healthy rats and further on animals bearing for instance the HCC tumor.

6.5.2 *Use of N-acetyl-[5-¹³C]-L-glutamine instead of [5-¹³C]-L-glutamine*

As described in previous Section 1.1 Glutamine instability and degradation, glutamine is very unstable in aqueous state and easily degrades to unwanted glutamic acid and pyroglutamic acid, however, its acetylated analogue N-acetyl-L-glutamine, does not. Due to the presence of acetyl group attached to amine group, N-acetyl-L-glutamine does not undergo reaction to pyroglutamic acid, and therefore is more stable. It has been shown to be stable in solution even after heat sterilization [123]. Study of the utilization of intravenously administered N-Acetyl-L-Glutamine in humans by Magnusson et.al. (1989) showed that Acetylglutamine concentration increased from undetectable values to 1,200±99 μmol/L after four hours of infusion. After 20 hours after the end of infusion; no acetylglutamine could be detected in plasma. The increase in plasma N-acetyl-L-glutamine level was accompanied by an increase in plasma glutamine concentration from 594±28 mmol/L to 728±26 mmol/L. A 25% to 35% increase in plasma glutamine was demonstrated in the studies, in which healthy subjects were given N-acetyl-L-glutamine [124].

Due to the fact that N-acetyl-[5-¹³C]-L-glutamine of better stability and the solubility is relatively same to L-glutamine, N-acetyl-L-glutamine is a possible candidate for DNP anf futher *in vivo* measurements. However, a study, which compares the metabolism of L-glutamine and N-acetyl-[5-¹³C]-L-glutamine must be performed first. The preparation protocol for N-acetyl-[5-¹³C]-L-glutamine for DNP can be alter to the one for L-glutamine.
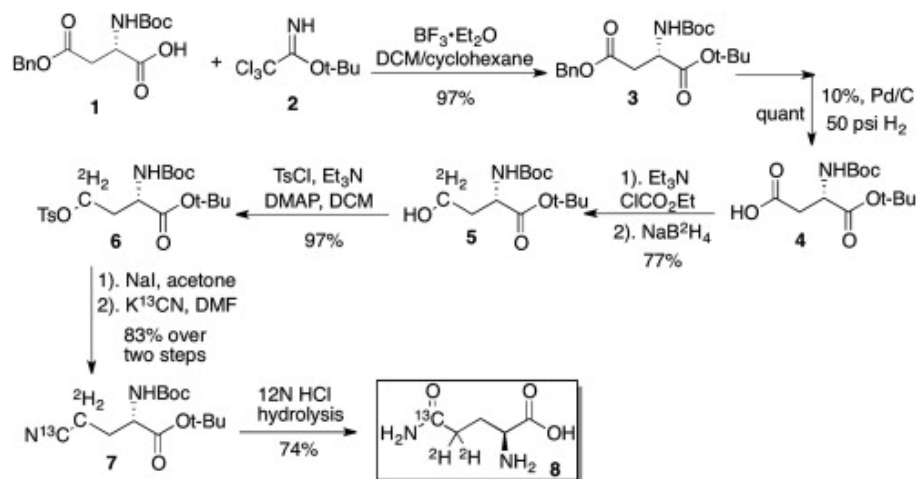
Figure 29: Synthesis of [5-¹³C-4-²H₂]-L-glutamine. Notation: 1) L-aspartic acid derivative, 2) tert-butyl tri-chloroacetimidate, 3) fully protected L-aspartic acid, 4) protected L-aspartic acid (except side chain), 5) 2-amino-4-hydroxybutanoic acid, 6) tosylate, 7) cyanide derivative, 8) [5-¹³C-4-²H₂]-L-glutamine [125].

6.5.3 *Use of [5-^{13}C-4-^{2}H$_2$]-L-Glutamine instead of [5-^{13}C]-L-glutamine*

A more promising approach is using [5-^{13}C-4-^{2}H$_2$]glutamine instead of [5-^{13}C]glutamine. Qu et. al. (2011) showed first example of using specifically deuterated [5-^{13}C-4-^{2}H$_2$]-L-glutamine in conjunction with hyperpolarized MRS. They were able to reach up to 10% hyperpolariaztion after 2 – 3 hours hyperpolarization with a measured T_1 of 33 s at 9.4 Tesla, whereas under the same condition, undeuterated [5-^{13}C]-L-glutamine showed at maximum T_1 values of less than half i. e. 15 s. The replacement of ^1H by ^2H atoms next to ^{13}C can substantially improve the T_1, therefore it would be very interesting to try this approach in the future [125].

The custom synthesis of [5-^{13}C-4-^{2}H$_2$]-L-glutamine could be easily repeated in our conditions. The synthesis was accomplished through a seven-step synthetic pathway with a 44% overall yield (see Fig 29). The introduction of two stable isotopes was performed by a NaB^{2}H$_4$-mixed anhydride reduction and K^{13}CN-nuclophilic substitution, respectively [125]. The desired [5-^{13}C-4-^{2}H$_2$]-L-glutamine was successfully obtained by a one-pot reaction of deprotection and controlled cyanide hydrolysis.

Part V

CONCLUSSION

"Don't be content in your life just to do no wrong.
Be prepared everyday to try and do some good."

— Sir Nicholas G. Winton

CONCLUSION

At the beginning of this thesis two goals have been set to be fulfill: (a) Optimize the hyperpolarization process of the [5-¹³C]-L-glutamine using Dynamic Nuclear Polarization (DNP) for further *in vivo* experiments. (b) Measure the enzymatic conversion of the [5-¹³C]-L-glutamine to [5-¹³C]glutamate using glutaminase *in vitro*. Due to the difficulties with the [5-¹³C]-L-glutamine liquid-state polarization loss during the transport, within the time scale of this master thesis only first aim could have been fulfilled.

However, we have described that nuclei like ¹⁴N and ¹³C with different γ ratios under unfavorable conditions, such as a short ¹⁴N-¹³C bond length (and strong J coupling), short T_1 of the ¹⁴N nucleus, and weak magnetic field, can engage in mutual relaxation. The fast polarization loss that occurs during the transfer of hyperpolarized amides to the MRI scanner is shown to be due to the scalar coupling contribution to relaxation at the low field that is present between the polarizer and scanner. Thus, the use of some amide-containing physiologically important metabolites, such as hyperpolarized DNP probes, might be impaired.

This phenomenon, although it has not been reported in literature previously, should be taken into account during the future design of next DNP-MRI laboratories. Either the polarizer should be located in the magnetic field of the MRI scanner, or better connected to the MRI scanner with a suitable sustained magnetic field transfer system.

The preparation technique described in this thesis is now prepared completely for further *in vitro* experiments using glutaminase and *in vivo* experiments on healthy and HCC-tumor bearing rats.

[1] L. Carroll, *Alice's adventures in wonderland.* Macmillan, 1865.

[2] E. Schulze and E. Bosshard, "Über das glutamin," *Berichte der deutschen chemischen Gesellschaft*, vol. 16, no. 1, pp. 312–315, 1883.

[3] R. G. Ham and W. L. McKeehan, "Media and growth requirements," *Methods Enzymol*, vol. 58, pp. 44–93, 1979.

[4] D. Darmaun, D. E. Matthews, and D. M. Bier, "Glutamine and glutamate kinetics in humans," *Am J Physiol*, vol. 251, pp. E117–26, Jul 1986.

[5] H. Eagle, "Nutrition needs of mammalian cells in tissue culture," *Science*, vol. 122, pp. 501–514, Sep 1955.

[6] T. C. Welbourne, "Interorgan glutamine flow in metabolic acidosis," *Am J Physiol*, vol. 253, pp. F1069–76, Dec 1987.

[7] R. E. Kimura, T. R. LaPine, J. Johnston, and J. Z. Ilich, "The effect of fasting on rat portal venous and aortic blood glucose, lactate, alanine, and glutamine," *Pediatr Res*, vol. 23, pp. 241–244, Feb 1988.

[8] G. Y. Wu and J. R. Thompson, "The effect of glutamine on protein turnover in chick skeletal muscle in vitro," *Biochem J*, vol. 265, pp. 593–598, Jan 1990.

[9] K. Horvath, M. Jami, I. D. Hill, J. C. Papadimitriou, L. S. Magder, and S. Chanasongcram, "Isocaloric glutamine-free diet and the morphology and function of rat small intestine," *JPEN J Parenter Enteral Nutr*, vol. 20, pp. 128–134, Mar-Apr 1996.

[10] D. W. Wilmore and J. K. Shabert, "Role of glutamine in immunologic responses," *Nutrition*, vol. 14, pp. 618–626, Jul-Aug 1998.

[11] J. Neu, V. Shenoy, and R. Chakrabarti, "Glutamine nutrition and metabolism: Where do we go from here?," *FASEB J*, vol. 10, pp. 829–837, Jun 1996.

[12] B. P. Bode, "Recent molecular advances in mammalian glutamine transport," *J Nutr*, vol. 131, pp. 2475S–85S; discussion 2486S–7S, Sep 2001.

[13] R. R. van der Hulst, B. K. van Kreel, M. F. von Meyenfeldt, R. J. Brummer, J. W. Arends, N. E. Deutz, and P. B. Soeters, "Glutamine and the preservation of gut integrity," *Lancet*, vol. 341, pp. 1363–1365, May 1993.

[14] B. J. Morlion, P. Stehle, P. Wachtler, H. P. Siedhoff, M. Koller, W. Konig, P. Furst, and C. Puchstein, "Total parenteral nutrition with glutamine dipeptide after major abdominal surgery: a randomized, double-blind, controlled study," *Ann Surg*, vol. 227, pp. 302–308, Feb 1998.

[15] C. B. Airaudo, A. Gayte-Sorbier, and P. Armand, "Stability of glutamine and pyroglutamic acid under model system conditions: influence of physical and technological factors," *Journal of Food Science*, vol. 52, no. 6, pp. 1750–1752, 1987.

[16] M. Sohn and C. Ho, "Ammonia generation during thermal degradation of amino acids," *Journal of agricultural and food chemistry*, vol. 43, pp. 3001–3003, 12 1995.

[17] L. Heller, A. Becher, A. Beck, and F. Muller, "On the problem of utilization of infused amino acid solutions.," *Klin Wochenschr*, vol. 45, pp. 317–318, Mar 1967.

[18] P. Stehle, P. Pfaender, and P. Fürst, "Isotachophoretic analysis of a synthetic dipeptide L-alanyl-L-glutamine. Evidence for stability during heat sterilization," *J. Chromatogr*, vol. 294, pp. 507–512, 1984.

[19] A. Gayte-Sorbier, C. B. Airaudo, and P. Armand, "Stability of glutamic acid and monosodium glutamate under model system conditions: Influence of physical and technological factors," *Journal of Food Science*, vol. 50, no. 2, pp. 350–352, 1985.

[20] K. Arii, H. Kobayashi, T. Kai, and Y. Kokuba, "Degradation kinetics of *l*-glutamine in aqueous solution," *Eur J Pharm Sci*, vol. 9, pp. 75–78, Oct 1999.

[21] F. W. Foreman, "The transformation of glutaminic acid into *l*-pyrrolidonecarboxylic acid in aqueous solution," *Biochem J*, vol. 8, pp. 481–493, Oct 1914.

[22] A. A. Mahdi, A. C. Rice, and K. G. Weckel, "Off-flavors in foods. Effect of pyrrolidonecarboxylic acid on flavor of processed fruit and vegetable products," *Journal Of Agricultural And Food Chemistry*, vol. 9, p. 143, 1961.

[23] F. M. Clydesdale, Y. D. Lin, and F. J. Francis, "Formation of 2-pyrrolidone-5-carboxylic acid from glutamine during processing and storage of spinach puree," *Journal of Food Science*, vol. 37, no. 1, pp. 45–47, 1972.

[24] T. E. Acree and C. Y. Lee, "A kinetic study of the cyclization of *l*-glutamine to 2-pyrrolidone-5-carboxylic acid in a model system," *Journal of Agricultural and Food Chemistry*, vol. 23, no. 4, pp. 828–830, 1975.

[25] F. F. SHIH, "Effect of anions on the deamidation of soy protein," *Journal of Food Science*, vol. 56, no. 2, pp. 452–454, 1991.

[26] H. T. Wright, "Nonenzymatic deamidation of asparaginyl and glutaminyl residues in proteins," *Crit Rev Biochem Mol Biol*, vol. 26, no. 1, pp. 1–52, 1991.

[27] J. Zhang, T. C. Lee, and C. T. Ho, "Comparative study on kinetics of nonenzymatic deamidation of soy protein and egg white lysozyme," *Journal of Agricultural and Food Chemistry*, vol. 41, no. 12, pp. 2286–2290, 1993.

[28] J. Hamada and W. Marshall, "Preparation and Functional Properties of Enzymatically Deamidated Soy Proteins," *Journal of Food Science*, vol. 54, no. 3, pp. 598–601, 1989.

[29] N. E. Robinson and A. B. Robinson, *Molecular clocks: Deamidation of asparaginyl and glutaminyl residues in peptides and proteins.* Althouse Press: Cave Junction, OR, 2004.

[30] W. W. Souba, R. J. Smith, and D. W. Wilmore, "Glutamine metabolism by the intestinal tract," *JPEN J Parenter Enteral Nutr*, vol. 9, pp. 608–617, Sep-Oct 1985.

[31] K. Khan, G. Hardy, B. McElroy, and M. Elia, "The stability of *l*-glutamine in total parenteral nutrition solutions," *Clin Nutr*, vol. 10, pp. 193–198, Aug 1991.

[32] D. Haussinger and F. Schliess, "Glutamine metabolism and signaling in the liver," *Front Biosci*, vol. 12, pp. 371–391, 2007.

[33] J. D. McGivan and C. I. Bungard, "The transport of glutamine into mammalian cells," *Front Biosci*, vol. 12, pp. 874–882, 2007.

[34] M. Pollard, D. Meredith, and J. D. McGivan, "Identification of a plasma membrane glutamine transporter from the rat hepatoma cell line H4-IIE-C3," *Biochem J*, vol. 368, pp. 371–375, Nov 2002.

[35] B. P. Bode, B. C. Fuchs, B. P. Hurley, J. L. Conroy, J. E. Suetterlin, K. K. Tanabe, D. B. Rhoads, S. F. Abcouwer, and W. W. Souba, "Molecular and functional analysis of glutamine uptake in human hepatoma and liver-derived cells," *Am J Physiol Gastrointest Liver Physiol*, vol. 283, pp. G1062–73, Nov 2002.

[36] M. S. Kilberg, M. E. Handlogten, and H. N. Christensen, "Characteristics of an amino acid transport system in rat liver for glutamine, asparagine, histidine, and closely related analogs," *Journal of Biological Chemistry*, vol. 255, no. 9, pp. 4011–9, 1980.

[37] S. Gu, H. L. Roderick, P. Camacho, and J. X. Jiang, "Identification and characterization of an amino acid transporter expressed differentially in liver," *Proceedings of the National Academy of Sciences*, vol. 97, no. 7, pp. 3230–3235, 2000.

[38] Y.-J. Fei, M. Sugawara, T. Nakanishi, W. Huang, H. Wang, P. D. Prasad, F. H. Leibach, and V. Ganapathy, "Primary structure, genomic organization, and functional and electrogenic characteristics of human system N 1, a Na^+- and H^+-coupled glutamine transporter," *Journal of Biological Chemistry*, vol. 275, no. 31, pp. 23707–23717, 2000.

[39] H. S. Hundal, M. J. Rennie, and P. W. Watt, "Characteristics of *l*-glutamine transport in perfused rat skeletal muscle," *The Journal of Physiology*, vol. 393, no. 1, pp. 283–305, 1987.

[40] A. M. Karinch, C.-M. Lin, C. L. Wolfgang, M. Pan, and W. W. Souba, "Regulation of expression of the SN1 transporter during renal adaptation to chronic metabolic acidosis in rats," *Am J Physiol Renal Physiol*, vol. 283, pp. F1011–9, Nov 2002.

[41] T. T. Solbu, J.-L. Boulland, W. Zahid, M. K. Lyamouri Bredahl, M. Amiry-Moghaddam, J. Storm-Mathisen, B. A. Roberg, and F. A. Chaudhry, "Induction and targeting of the glutamine transporter SN1 to the basolateral membranes of cortical kidney tubule cells during chronic metabolic acidosis suggest a role in pH regulation," *J Am Soc Nephrol*, vol. 16, pp. 869–877, Apr 2005.

[42] B. K. Tamarappoo, M. K. Raizada, and M. S. Kilberg, "Identification of a system N-like Na(+)-dependent glutamine transport activity in rat brain neurons," *J Neurochem*, vol. 68, pp. 954–960, Mar 1997.

[43] F. A. Chaudhry, R. J. Reimer, D. Krizaj, D. Barber, J. Storm-Mathisen, D. R. Copenhagen, and R. H. Edwards, "Molecular analysis of system N suggests novel physiological roles in nitrogen metabolism and synaptic transmission," *Cell*, vol. 99, pp. 769–780, Dec 1999.

[44] B. P. Bode, D. L. Kaminski, W. W. Souba, and A. P. Li, "Glutamine transport in isolated human hepatocytes and transformed liver cells," *Hepatology*, vol. 21, pp. 511–520, Feb 1995.

[45] C. Lenzen, S. Soboll, H. Sies, and D. Haussinger, "pH control of hepatic glutamine degradation. Role of transport," *Eur J Biochem*, vol. 166, pp. 483–488, Jul 1987.

[46] F. A. Chaudhry, D. Krizaj, P. Larsson, R. J. Reimer, C. Wreden, J. Storm-Mathisen, D. Copenhagen, M. Kavanaugh, and R. H. Edwards, "Coupled and uncoupled proton movement by amino acid transport system N," *EMBO J*, vol. 20, pp. 7041–7051, Dec 2001.

[47] A. Broer, A. Albers, I. Setiawan, R. H. Edwards, F. A. Chaudhry, F. Lang, C. A. Wagner, and S. Broer, "Regulation of the glutamine transporter SN1 by extracellular pH and intracellular sodium ions," *J Physiol*, vol. 539, pp. 3–14, Feb 2002.

[48] T. Nakanishi, M. Sugawara, W. Huang, R. G. Martindale, F. H. Leibach, M. E. Ganapathy, P. D. Prasad, and V. Ganapathy, "Structure, function, and tissue expression pattern of human SN2, a subtype of the amino acid transport system N," *Biochem Biophys Res Commun*, vol. 281, pp. 1343–1348, Mar 2001.

[49] F. E. Baird, K. J. Beattie, A. R. Hyde, V. Ganapathy, M. J. Rennie, and P. M. Taylor, "Bidirectional substrate fluxes through the system N (SNAT5) glutamine transporter may determine net glutamine flux in rat liver," *J Physiol*, vol. 559, pp. 367–381, Sep 2004.

[50] R. J. Reimer, F. A. Chaudhry, A. T. Gray, and R. H. Edwards, "Amino acid transport System A resembles System N in sequence but differs in mechanism," *Proceedings of the National Academy of Sciences*, vol. 97, no. 14, pp. 7715–7720, 2000.

[51] M. Sugawara, T. Nakanishi, Y.-J. Fei, W. Huang, M. E. Ganapathy, F. H. Leibach, and V. Ganapathy, "Cloning of an amino acid transporter with functional characteristics and tissue expression pattern identical to that of system A," *Journal of Biological Chemistry*, vol. 275, no. 22, pp. 16473–16477, 2000.

[52] D. Yao, B. Mackenzie, H. Ming, H. Varoqui, H. Zhu, M. A. Hediger, and J. D. Erickson, "A novel system A isoform mediating Na^+/neutral amino acid cotransport," *Journal of Biological Chemistry*, vol. 275, no. 30, pp. 22790–22797, 2000.

[53] T. Hatanaka, W. Huang, H. Wang, M. Sugawara, P. D. Prasad, F. H. Leibach, and V. Ganapathy, "Primary structure, functional characteristics and tissue expression pattern of human ATA2, a subtype of amino acid transport system A," *Biochim Biophys Acta*, vol. 1467, pp. 1–6, Jul 2000.

[54] H. Varoqui, H. Zhu, D. Yao, H. Ming, and J. D. Erickson, "Cloning and functional identification of a neuronal glutamine transporter," *Journal of Biological Chemistry*, vol. 275, no. 6, pp. 4049–4054, 2000.

[55] R. Lohmann, W. W. Souba, and B. P. Bode, "Rat liver endothelial cell glutamine transporter and glutaminase expression contrast with parenchymal cells," *American Journal of Physiology - Gastrointestinal and Liver Physiology*, vol. 276, no. 3, pp. G743–G750, 1999.

[56] R. Kekuda, V. Torres-Zamorano, Y. J. Fei, P. D. Prasad, H. W. Li, L. D. Mader, F. H. Leibach, and V. Ganapathy, "Molecular and functional characterization of intestinal Na(+)-dependent neutral amino acid transporter B0," *American Journal of Physiology - Gastrointestinal and Liver Physiology*, vol. 272, no. 6, pp. G1463–G1472, 1997.

[57] R. Kekuda, P. D. Prasad, Y. J. Fei, V. Torres-Zamorano, S. Sinha, T. L. Yang-Feng, F. H. Leibach, and V. Ganapathy, "Cloning of the sodium-dependent, broad-scope, neutral amino acid transporter Bo from a human placental choriocarcinoma cell line," *J Biol Chem*, vol. 271, pp. 18657–18661, Aug 1996.

[58] V. Torres-Zamorano, F. H. Leibach, and V. Ganapathy, "Sodium-dependent homo- and hetero-exchange of neutral amino acids mediated by the amino acid transporter ATB degree," *Biochem Biophys Res Commun*, vol. 245, pp. 824–829, Apr 1998.

[59] A. Broer, N. Brookes, V. Ganapathy, K. S. Dimmer, C. A. Wagner, F. Lang, and S. Broer, "The astroglial ASCT2 amino acid transporter as a mediator of glutamine efflux," *J Neurochem*, vol. 73, pp. 2184–2194, Nov 1999.

[60] N. Utsunomiya-Tate, H. Endou, and Y. Kanai, "Cloning and functional characterization of a System ASC-like Na^+-dependent neutral amino acid transporter," *Journal of Biological Chemistry*, vol. 271, no. 25, pp. 14883–14890, 1996.

[61] D. Torrents, R. Estévez, M. Pineda, E. Fernández, J. Lloberas, Y.-B. Shi, A. Zorzano, and M. PalacÆ±ÃÅn, "Identification and characterization of a membrane protein (y$^+$L amino acid transporter-1) that associates with 4F2hc to Encode the Amino Acid Transport Activity y$^+$L," *Journal of Biological Chemistry*, vol. 273, no. 49, pp. 32437–32445, 1998.

[62] A. Broer, C. Wagner, F. Lang, and S. Broer, "Neutral amino acid transporter ASCT2 displays substrate-induced Na+ exchange and a substrate-gated anion conductance," *Biochem J*, vol. 346 Pt 3, pp. 705–710, Mar 2000.

[63] Y. Kanai, "Family of neutral and acidic amino acid transporters: molecular biology, physiology and medical implications," *Curr Opin Cell Biol*, vol. 9, pp. 565–572, Aug 1997.

[64] F. Oppedisano, L. Pochini, M. Galluccio, M. Cavarelli, and C. Indiveri, "Reconstitution into liposomes of the glutamine/amino acid transporter from renal cell plasma membrane: functional characterization, kinetics and activation by nucleotides," *Biochim Biophys Acta*, vol. 1667, pp. 122–131, Dec 2004.

[65] H. A. Krebs, "Metabolism of amino-acids: The synthesis of glutamine from glutamic acid and ammonia, and the enzymic hydrolysis of glutamine in animal tissues," *Biochem J*, vol. 29, pp. 1951–1969, Aug 1935.

[66] M. Watford, "Hepatic glutaminase expression: Relationship to kidney-type glutaminase and to the urea cycle," *FASEB J*, vol. 7, pp. 1468–1474, Dec 1993.

[67] J. Hoek, R. Charles, E. D. Haan, and J. Tager, "Glutamate oxidation in rat-liver homogenate," *Biochimica et Biophysica Acta (BBA) - Bioenergetics*, vol. 172, no. 3, pp. 407 – 416, 1969.

[68] S. K. Joseph and J. D. McGivan, "The effect of ammonium chloride and glucagon on the metabolism of glutamine in isolated liver cells from starved rats," *Biochim Biophys Acta*, vol. 543, pp. 16–28, Sep 1978.

[69] J. D. McGivan and N. M. Bradford, "Characteristics of the activation of glutaminase by ammonia in sonicated rat liver mitochondria," *Biochim Biophys Acta*, vol. 759, pp. 296–302, Sep 1983.

[70] D. Haussinger and H. Sies, "Hepatic glutamine metabolism under the influence of the portal ammonia concentration in the perfused rat liver," *Eur J Biochem*, vol. 101, pp. 179–184, Nov 1979.

[71] A. F. Moorman, P. A. de Boer, M. Watford, M. A. Dingemanse, and W. H. Lamers, "Hepatic glutaminase mrna is confined to part of the urea cycle domain in the adult rodent liver lobule.," *FEBS Lett*, vol. 356, pp. 76–80, Dec 1994.

[72] A. P. Halestrap, "The regulation of the matrix volume of mammalian mitochondria in vivo and in vitro and its role in the control of mitochondrial metabolism," *Biochim Biophys Acta*, vol. 973, pp. 355–382, Mar 1989.

[73] B. P. Bode and W. W. Souba, "Modulation of cellular proliferation alters glutamine transport and metabolism in human hepatoma cells," *Ann Surg*, vol. 220, pp. 411–422, Oct 1994.

[74] D. Anastasiou and L. C. Cantley, "Breathless cancer cells get fat on glutamine," *Cell Res*, vol. 22, pp. 443–446, Mar 2012.

[75] M. G. Vander Heiden, L. C. Cantley, and C. B. Thompson, "Understanding the Warburg effect: the metabolic requirements of cell proliferation," *Science*, vol. 324, pp. 1029–1033, May 2009.

[76] C. L. Collins, M. Wasa, W. W. Souba, and S. F. Abcouwer, "Determinants of glutamine dependence and utilization by normal and tumor-derived breast cell lines," *J Cell Physiol*, vol. 176, pp. 166–178, Jul 1998.

[77] M. A. Medina, F. Sanchez-Jimenez, J. Marquez, A. Rodriguez Quesada, and I. Nunez de Castro, "Relevance of glutamine metabolism to tumor cell growth," *Mol Cell Biochem*, vol. 113, pp. 1–15, Jul 1992.

[78] L. J. Reitzer, B. M. Wice, and D. Kennell, "Evidence that glutamine, not sugar, is the major energy source for cultured HeLa cells," *J Biol Chem*, vol. 254, pp. 2669–2676, Apr 1979.

[79] M. Wasa, H.-S. Wang, and A. Okada, "Characterization of L-glutamine transport by a human neuroblastoma cell line," *Am J Physiol Cell Physiol*, vol. 282, pp. C1246–53, Jun 2002.

[80] D. R. Wise, R. J. DeBerardinis, A. Mancuso, N. Sayed, X.-Y. Zhang, H. K. Pfeiffer, I. Nissim, E. Daikhin, M. Yudkoff, S. B. McMahon, and C. B. Thompson, "Myc regulates a transcriptional program that stimulates mitochondrial glutaminolysis and leads to glutamine addiction," *Proceedings of the National Academy of Sciences*, vol. 105, no. 48, pp. 18782–18787, 2008.

[81] B. P. Bode, N. Reuter, J. L. Conroy, and W. W. Souba, "Protein kinase C regulates nutrient uptake and growth in hepatoma cells," *Surgery*, vol. 124, pp. 260–267, Aug 1998.

[82] T. M. Pawlik, W. W. Souba, T. J. Sweeney, and B. P. Bode, "Phorbol esters rapidly attenuate glutamine uptake and growth in human colon carcinoma cells," *J Surg Res*, vol. 90, pp. 149–155, May 2000.

[83] W. W. Souba, M. Pan, and B. R. Stevens, "Kinetics of the sodium-dependent glutamine transporter in human intestinal cell confluent monolayers," *Biochem Biophys Res Commun*, vol. 188, pp. 746–753, Oct 1992.

[84] C. I. Bungard and J. D. McGivan, "Glutamine availability up-regulates expression of the amino acid transporter protein ASCT2 in HepG2 cells and stimulates the ASCT2 promoter," *Biochem J*, vol. 382, pp. 27–32, Aug 2004.

[85] P. Gao, I. Tchernyshyov, T.-C. Chang, Y.-S. Lee, K. Kita, T. Ochi, K. I. Zeller, A. M. De Marzo, J. E. Van Eyk, J. T. Mendell, and C. V. Dang, "c-Myc suppression of miR-23a/b enhances mitochondrial glutaminase expression and glutamine metabolism," *Nature*, vol. 458, pp. 762–765, Apr 2009.

[86] K. N. Rajagopalan and R. J. DeBerardinis, "Role of glutamine in cancer: Therapeutic and imaging implications," *J Nucl Med*, vol. 52, pp. 1005–1008, Jul 2011.

[87] C. M. Metallo, P. A. Gameiro, E. L. Bell, K. R. Mattaini, J. Yang, K. Hiller, C. M. Jewell, Z. R. Johnson, D. J. Irvine, L. Guarente, J. K. Kelleher, M. G. Vander Heiden, O. Iliopoulos, and G. Stephanopoulos, "Reductive glutamine metabolism by IDH1 mediates lipogenesis under hypoxia," *Nature*, vol. 481, pp. 380–384, 01 2012.

[88] J. Kurhanewicz, D. B. Vigneron, K. Brindle, E. Y. Chekmenev, A. Comment, C. H. Cunningham, R. J. Deberardinis, G. G. Green, M. O. Leach, S. S. Rajan, R. R. Rizi, B. D. Ross, W. S. Warren, and C. R. Malloy, "Analysis of cancer metabolism by imaging hyperpolarized nuclei: prospects for translation to clinical research," *Neoplasia*, vol. 13, pp. 81–97, Feb 2011.

[89] F. Gallagher, M. Kettunen, and K. Brindle, "Biomedical applications of hyperpolarized ^{13}C magnetic resonance imaging," *Progress in Nuclear Magnetic Resonance Spectroscopy*, vol. 55, no. 4, pp. 285–295, 2009.

[90] W. A. Edelstein, G. H. Glover, C. J. Hardy, and R. W. Redington, "The intrinsic signal-to-noise ratio in NMR imaging," *Magn Reson Med*, vol. 3, pp. 604–618, Aug 1986.

[91] N. G. Campeau, J. r. Huston, M. A. Bernstein, C. Lin, and G. F. Gibbs, "Magnetic resonance angiography at 3.0 Tesla: initial clinical experience," *Top Magn Reson Imaging*, vol. 12, pp. 183–204, Jun 2001.

[92] D. G. Gadian and G. K. Radda, "NMR studies of tissue metabolism," *Annu Rev Biochem*, vol. 50, pp. 69–83, 1981.

[93] J. Kurhanewicz and D. B. Vigneron, "Advances in MR spectroscopy of the prostate," *Magn Reson Imaging Clin N Am*, vol. 16, pp. 697–710, Nov 2008.

[94] S. J. Nelson, E. Graves, A. Pirzkall, X. Li, A. Antiniw Chan, D. B. Vigneron, and T. R. McKnight, "In vivo molecular imaging for planning radiation therapy of gliomas: An application of ^{1}H MRSI," *Journal of Magnetic Resonance Imaging*, vol. 16, no. 4, pp. 464–476, 2002.

[95] F. Sardanelli, A. Fausto, and F. Podo, "MR spectroscopy of the breast," *Radiol Med*, vol. 113, pp. 56–64, Feb 2008.

[96] M. van der Graaf, "In vivo magnetic resonance spectroscopy: Basic methodology and clinical applications," *Eur Biophys J*, vol. 39, pp. 527–540, Mar 2010.

[97] K. Coyne, "Mri: A guided tour."

[98] K. Golman, L. E. Olsson, O. Axelsson, S. Mansson, M. Karlsson, and J. S. Petersson, "Molecular imaging using hyperpolarized ^{13}C," *Br J Radiol*, vol. 76 Spec No 2, pp. S118–27, 2003.

[99] G. Frossati, "Polarization of ^{3}He, D_2 (and possibly ^{129}Xe) using cryogenic techniques," *Nuclear Instruments and Methods in Physics Research Section A: Accelerators, Spectrometers, Detectors and Associated Equipment*, vol. 402, pp. 479–483, 1 1998.

[100] Bowers and Weitekamp, "Transformation of symmetrization order to nuclear-spin magnetization by chemical reaction and nuclear magnetic resonance," *Phys Rev Lett*, vol. 57, pp. 2645–2648, Nov 1986.

[101] P. Bhattacharya, E. Y. Chekmenev, W. H. Perman, K. C. Harris, A. P. Lin, V. A. Norton, C. T. Tan, B. D. Ross, and D. P. Weitekamp, "Towards hyperpolarized ^{13}C-succinate imaging of brain cancer," *Journal of Magnetic Resonance*, vol. 186, pp. 150–155, 5 2007.

[102] M. A. Bouchiat, T. R. Carver, and C. M. Varnum, "Nuclear polarization in He^3 gas induced by optical pumping and dipolar exchange," *Phys. Rev. Lett.*, vol. 5, pp. 373–375, Oct 1960.

[103] B. C. Grover, "Noble-gas NMR detection through noble-gas-rubidium hyperfine contact interaction," *Phys. Rev. Lett.*, vol. 40, pp. 391–392, Feb 1978.

[104] M. S. Albert, G. D. Cates, B. Driehuys, W. Happer, B. Saam, C. S. Springer, and A. Wishnia, "Biological magnetic resonance imaging using laser-polarized ^{129}Xe," *Nature*, vol. 370, pp. 199–201, 07 1994.

[105] K. Golman, J. S. Petersson, J. H. Ardenkjaer-Larsen, I. Leunbach, L. G. Wistrand, G. Ehnholm, and K. Liu, "Dynamic in vivo oxymetry using overhauser enhanced MR imaging," *J Magn Reson Imaging*, vol. 12, pp. 929–938, Dec 2000.

[106] B. M. Goodson, "Nuclear magnetic resonance of laser-polarized noble gases in molecules, materials, and organisms," *Journal of Magnetic Resonance*, vol. 155, no. 2, pp. 157 – 216, 2002.

[107] A. W. Overhauser, "Polarization of nuclei in metals," *Phys. Rev.*, vol. 92, pp. 411–415, Oct 1953.

[108] T. R. Carver and C. P. Slichter, "Polarization of nuclear spins in metals," *Phys. Rev.*, vol. 92, pp. 212–213, Oct 1953.

[109] J. Heckmann, W. Meyer, E. Radtke, G. Reicherz, and S. Goertz, "Electron spin resonance and its implication on the maximum nuclear polarization of deuterated solid target materials," *Physical Review B*, vol. 74, pp. 134418–, 10 2006.

[110] J. H. Ardenkjaer-Larsen, B. Fridlund, A. Gram, G. Hansson, L. Hansson, M. H. Lerche, R. Servin, M. Thaning, and K. Golman, "Increase in signal-to-noise ratio of $> 10,000$ times in liquid-state NMR," *Proc Natl Acad Sci U S A*, vol. 100, pp. 10158–10163, Sep 2003.

[111] W. Boer, M. Borghini, K. Morimoto, T. O. Niinikoski, and F. Udo, "Dynamic polarization of protons, deuterons, and carbon-13 nuclei: Thermal contact between nuclear spins and an electron spin-spin interaction reservoir," vol. 15, no. 3-4, pp. 249–267, 1974.

[112] W. de Boer and T. O. Niinikoski, "Dynamic proton polarization in propanediol below 0.5 K," *Nuclear Instruments and Methods*, vol. 114, pp. 495–498, 2 1974.

[113] J. H. Ardenkjaer-Larsen, S. Macholl, and H. Jóhannesson, "Dynamic nuclear polarization with trityls at 1.2 k," vol. 34, no. 3-4, pp. 509–522, 2008.

[114] J. H. Ardenkjaer-Larsen, "^{13}C Hyperpolarization: Imaging of Agents Pre-polarized by the DNP-NMR Method," *in ISMRM presentation*, 2005.

[115] K. M. Brindle, S. E. Bohndiek, F. A. Gallagher, and M. I. Kettunen, "Tumor imaging using hyperpolarized ^{13}C magnetic resonance spectroscopy," *Magn Reson Med*, vol. 66, pp. 505–519, Aug 2011.

[116] F. A. Gallagher, M. I. Kettunen, S. E. Day, M. Lerche, and K. M. Brindle, "^{13}C MR spectroscopy measurements of glutaminase activity in human hepatocellular carcinoma cells using hyperpolarized ^{13}C-labeled glutamine," *Magn Reson Med*, vol. 60, pp. 253–257, Aug 2008.

[117] J. Becker, R. R. Shoup, and T. C. Farrar, "^{13}C NMR spectroscopy: relaxation times of ^{13}C and methods for sensitivity enhancement," *Pure Appl. Chem*, vol. 32, pp. 51–66, 1972.

[118] P. Mieville, S. Jannin, and G. Bodenhausen, "Relaxometry of insensitive nuclei: optimizing dissolution dynamic nuclear polarization," *J Magn Reson*, vol. 210, pp. 137–140, May 2011.

[119] E. Chiavazza, E. Kubala, C. V. Gringeri, S. Düwel, M. Durst, R. F. Schulte, and M. I. Menzel, "Earth's magnetic field enabled scalar coupling relaxation of ^{13}C nuclei bound to fast-relaxing quadrupolar ^{14}N in amide groups," *Journal of Magnetic Resonance*, no. 0, pp. –, 2012.

[120] S. D. for Organic Compounds SDBS, "February 2013 `http://sdbs.riodb.aist.go.jp`."

[121] KEGG, "D-Glutamine and D-glutamate metabolism. January 2013 `http://www.genome.jp/kegg/`."

[122] C. Cabella, M. Karlsson, C. Canapè, G. Catanzaro, S. Colombo Serra, L. Miragoli, L. Poggi, F. Uggeri, L. Venturi, P. R. Jensen, M. H. Lerche, and F. Tedoldi, "In vivo and in vitro liver cancer metabolism observed with hyperpolarized [5-13c]glutamine," *Journal of Magnetic Resonance*, vol. 232, pp. 45–52, 7 2013.

[123] M. K. Snowden, J. H. Baxter, M. Mamula Bergana, I. Reyzer, and V. Pound, "Stability of n-acetylglutamine and glutamine in aqueous solution and in a liquid nutritional product by an improved hplc method," *Journal of Food Science*, vol. 67, no. 1, pp. 384–389, 2002.

[124] A. Arnaud, M. Ramirez, J. H. J. H. Baxter, and A. J. A. J. Angulo, "Absorption of enterally administered N-acetyl-*l*-glutamine versus glutamine in pigs," *Clin Nutr*, vol. 23, pp. 1303–1312, Dec 2004.

[125] W. Qu, Z. Zha, B. P. Lieberman, A. Mancuso, M. Stetz, R. Rizzi, K. Ploessl, D. Wise, C. Thompson, and H. F. Kung, "Facile synthesis [5-^{13}C-4-^{2}H$_2$]-L-glutamine for hyperpolarized MRS imaging of cancer cell metabolism," *Acad Radiol*, vol. 18, pp. 932–939, Aug 2011.